JOURNAL OF APPLIED ELECTROCHEMISTRY **28** (1998) 759–780

REVIEWS IN APPLIED ELECTROCHEMISTRY NUMBER 49

The rotating cylinder electrode: its continued development and application*

D. R. GABE, G. D. WILCOX

IPTME, Loughborough University of Technology, Loughborough, LE11 3TU, Great Britain

J. GONZALEZ-GARCIA‡ and F. C. WALSH

Division of Chemistry, Portsmouth University, Portsmouth, PO1 2DT, Great Britain

Received 10 December 1996; revised 22 December 1997

The application of rotating cylinder electrodes (RCEs) in electrochemistry has been reviewed for the period 1982–1995. Among the applications highlighted are the novel design of cell geometries and reactors for a range of electrochemical processes, voltammetry and analysis, electrodeposition and corrosion. This range amply indicates the widespread acceptance of the RCE for studies in a number of interdisciplinary fields.

Keywords: *rotating cylinder*, *rotating cylinder reactors*, *environmental treatment*, *mass transport*, *surface roughness*

Symbols and nomenclature

RCE	rotating cylinder electrode
RConE	rotating cone electrode
RDE	rotating disc electrode
RHSE	rotating hemispherical electrode
	saturated calomel electrode
Re	Reynolds number $= Ud/v$
Sc	Schmidt number $= v/D$
Sh	Sherwood number $= k_m d/D$
Le	dimensionless length group $= h/d$
Wa	Wagner number $= (d\eta/di)(\kappa/L)$
a, b, c	power indice constants
A	active electrode surface area (cm^2)
C	concentration ($mol\,cm^{-3}$)
d	cylinder diameter (cm)
D	diffusion coefficient ($cm^2\,s^{-1}$)
F	Faraday's constant ($96\,485\,A\,s\,mol^{-1}$)
h	Surface roughness of RCE (cm)
i_L	limiting current density ($A\,cm^{-2}$)
I_L	limiting current (A)
K	correlation constant
k_m	mass transport coefficient $= i_L/zFC$ ($cm\,s^{-1}$)
l	characteristic length (of cylinder) (cm)
L	characteristic length (in Wagner number) (cm)
Q	volumetric flow rate ($cm^3\,s^{-1}$)
U	rotational velocity ($cm\,s^{-1}$)
V_T	volume of electrolyte in the tank (cm^3)
z	number of electrons, electron change
ϵ	height protruberance, roughness (cm)
v	kinematic viscosity ($cm^2\,s^{-1}$)
γ	degree of enhancement
η	overpotential (V)
κ	solution conductivity ($S\,cm^{-1}$)
$\overline{\omega}$	angular velocity ($rad\,s^{-1}$)

1. Introduction

Electrodes have been rotated at least since 1905 to provide some quantitative control of solution convection. Hydrodynamic theory for such electrode is generally considered to originate with Levich [1] although in practice this was limited to the rotating disc electrode which, to this day, remains the best-known geometry employed. Updating reviews have appeared at regular intervals [2–6] and a number of other geometries have been explored (see Fig. 1), namely the rotating cylinder electrode, rotating cone electrode, rotating hemispherical electrode, but only the RCE has grown to be generally accepted and increasingly widely used. If characteristics are studied it can quickly be seen that the RDE and RCE are limiting examples of truncated geometries and the RConE and RHSE are intermediates which are more like the RDE, characterized by predominant laminar flow, while the RCE is characterized by turbulent flow. Using the Reynolds number as transition criterion ($Re = Ud/v$), the Sherwood number as a mass

* **In memoriam**: This paper is dedicated to the memory of Professor Charles Tobias who died early in 1996. Among his many contributions to electrochemical engineering, we have particularly appreciated the papers on mass transport to rotating cylinders which have provided the basis for many succeeding studies and the portfolio of research reported in this review.

‡ On leave from Departamento Quimica-Fisica, Universidad de Alicante, AP Correos 99, 03080, Alicante, Spain.

0021-891X

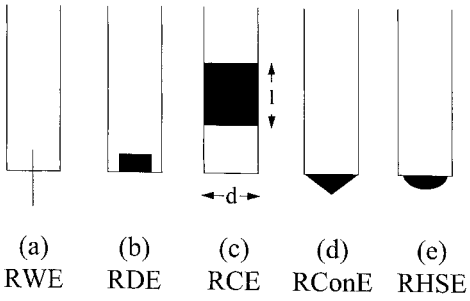

Fig. 1. Common types of laboratory rotating electrodes: (a) rotating wire electrode (RWE), (b) rotating disc electrode (RDE), (c) rotating cylinder electrode (RCE), (d) rotating cone electrode (RCOnE) and (e) rotating hemispherical electrode (RHSE).

transport coefficient in the correlation $Sh \propto Re^n$ this can be easily noted as indicated in Table 1.

Variants have been studied (e.g., rotating ring disc electrode) and external flows superimposed (e.g., jetting), for which mass transfer correlations are now well-established. Since 1970 research has been concerned primarily with using the systems as electrochemical tools and fundamental research has been concerned with subtleties of the systems (e.g., Taylor vortices for the RCE cell) and simulation theory between fluid flow and rotational convective flow.

Electrochemical mass transfer studies are dependent upon measurement of the limiting current density, as the diffusive ion flux to or from the electrode surface. This subject is considered to be beyond the scope of this paper, although there are a number of recent reviews [7–11].

This review follows earlier reviews [12, 13] and, in particular, seeks to survey areas which have been explored and developed since 1983 and to describe applications which have established new opportunities for electrochemical techniques. However, it is worth repeating the main features of the RCE which give it unique experimental characteristics. These are:

(a) It generates turbulent convection at $Re > 100$, thereby providing simulation conditions of this type of convection at relatively low rotation rates.
(b) The potential and current densities are substantially uniform thereby promoting uniform reaction rates over the cathode surface.
(c) Mass transport is high and can be further enhanced through development or use of roughened surfaces.
(d) The mass transfer equations are well-established.
(e) Superimposed axial flow does not usually alter the mass transfer control.
(f) The most convenient design utilizes a rotating inner cylindrical electrode with a concentric outer counter electrode but the converse is possible. The active (working) electrode may be either cathode or anode.

The implications and exploitable advantages of each of these features will be described and discussed in this paper.

Table 1. Coefficients in the RCE Mass Transport Correlation Equation.

Geometry	*n(laminar)*	*n(turbulent)*	*Re(crit)*
RDE	0.5	0.8	1×10^5
RConE	0.45	0.90	2×10^4
RHSE	0.5	0.67	1×10^4
RCE	0.33	0.67	2×10^2
(Annulus	0.33	0.58	2×10^3)

2. Fluid flow

Ohba and Kuroda have provided a numerical analysis of flow around rotating circular and rotating square cylinders [14]. Body-fitted grid generation with a moving boundary technique was used to obtain solutions to the incompressible form of the Navier–Stokes equations. Periodical flows were predicted when the von Karman vortex shedding and the rotation of the cylinder were synchronized.

The rapid development of computational methods has greatly advanced calculations in fluid dynamics but experimental methods to obtain spatial velocity information have appeared much more slowly. In the case of an inner concentric rotating cylinder in Taylor–Couette flow, [15] Takeda *et al.* [16] have deconvoluted a time-dependent velocity field using an ultrasonic Doppler velocity profile method. The Couette system involved an inner rotating cylinder of radius of 94 mm, an outer (static) cylinder radius of 104 mm and a length of 200 mm. The technique resulted in the appearance of an MWV (modulated wavy vortex flow field). MWV had not shown up clearly in previous studies of a rotating inner cylinder but has been observed in a counter-rotating Couette system [17].

The elegance and power of electrochemical techniques for flow characterization are evident in another study of Taylor–Couette flow [18] which uses a three-segment diffusion problem (Fig. 2). The probe, flush mounted in the walls of the outer cylinder, allowed azimuthal and axial components of shear rate [19] to be simultaneously monitored. The fluid was contained between two plexiglass cylinders of length 140 mm. The outer cylinder was of fixed radius, 30.6 mm, while inner cylinders of 28.8, 25.6 and 21.4 mm were used. Typically 28–15 vortices could be accommodated in the rotation speed range 0.6 to 36 rpm with an axial velocity of approximately 0.08 mm s^{-1}. These studies of instabilities in Taylor–Couette flow have recently been extended to non-Newtonian viscoelastic liquids [20].

3. Mass transport and its enhancement

The high rates of convective–diffusion mass transport experienced by RCE microelectrodes are considered later in Section 5. Here, two and three dimensional macro RCEs are considered. The prediction and

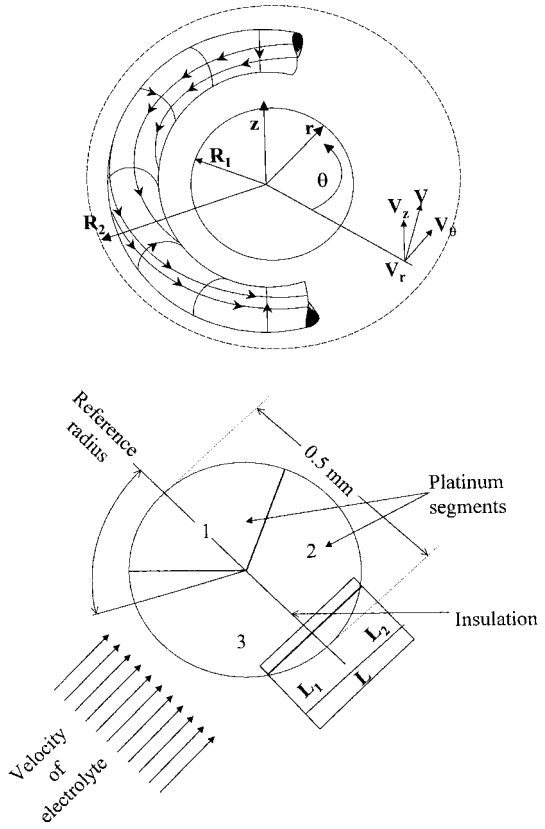

Fig. 2. Characterization of Taylor-Couette fluid flow: (a) structure of a Taylor vortex for flow stream tube and three-segment electrodiffusion probe; (b) expanded view of three-segment probe.

measurement of mass transport in RCEs continues to attract interest for several reasons [21–24]:

(i) In metal and polymer electrodeposition applications, the maximum rate of plating depends on the limiting current density at the electrode surface.
(ii) In environmental applications, the mass transport performance of an RCE will govern the rate of removal of a toxic solution species such as heavy metal ions.
(iii) For batch electrosynthesis, the achievement of a high reactant conversion in a reasonable electrolysis time requires a high rate of mass transport.
(iv) In the laboratory, controlled-potential coulometry studies using exhaustive electrolysis techniques again require high mass transport (an/or electrode area) to maintain a short analysis time.
(v) Mass transport to or from an inner RCE can be altered/controlled by a diverse number of factors including predetermined surface roughness or developing roughness (as in the case of deposition of roughened deposits or anodic formation of corrosion pits).

It was noted in a previous review [13] that mass transport to an inner RCE in turbulent flow may be described by empirical dimensionless correlations of the form:

$$Sh = K\ Re^{a}\ Sc^{b} \tag{1}$$

where the Sherwood, Reynolds and Schmidt numbers describe mass transport, fluid flow, and transport properties of the electrolyte.

Some authors have derived a value for $b = 0.356$ [13, 24–27] giving

$$Sh = K\ Re^{a}\ Sc^{0.356} \tag{2}$$

This correlation may be rewritten in terms of a dimensionless length group, $Le = h/d$ where h is a surface roughness and d is the diameter of the RCE:

$$Sh = K\ Re^{a}\ Sc^{0.356}\ Le^{c} \tag{3}$$

Examples of empirical correlations of this form are shown in Fig. 3 and Table 2. The constants K and a depend on (i) the type of roughness [28, 29], (ii) the degree of roughness [28–30] and (iii) the electrolyte composition, its temperature and the morphology of the metal deposit [31, 32].

Expansion of the dimensionless group in Equation 2 yields

$$\frac{k_{m}d}{D} = \frac{Ud^{a}}{v}\frac{v^{0.356}}{D} \tag{4}$$

where the characteristic length in Sh and Re is the rotating cylinder electrode diameter [13, 25] and the peripheral velocity is used as the characteristic velocity in Re [13, 25, 26, 28].

The active rotating cylinder electrode area is

$$A = \pi dl \tag{5}$$

which allows Equation 4 to be rewritten as

$$k_{m}A = KlU^{a}d^{a(0.356\text{-}a)}D^{0.644} \tag{6}$$

The performance of the RCE therefore depends upon the following:

(i) the size of the cathode (i.e. length and diameter)
(ii) the peripheral velocity of the RCE which is related to the rotation speed, and the diameter:

$$U = \omega\pi d \tag{7}$$

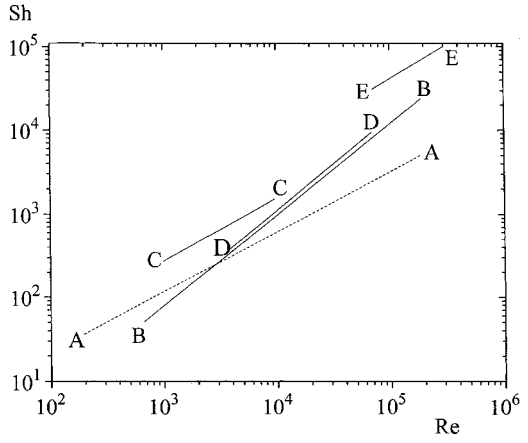

Fig. 3. Dimensionless group correlation of mass transport data for RCEs. A plot of Sherwood number against Reynolds number is shown for various types of roughness according to Equation 3 and Table 2.

Table 2. Dimensionless group mass transport correlations for various RCEs according to Expression 3

	Type of surface	*Re range*	*K*	*a*	*c*
A	Smooth	210–240 000	0.079	0.70	0
B	Knurled (staggered) diamond pyramids	600–250 000	1	1	−2
C	Longitudinal fins	1050–10 500	0.714	0.61	−0.2
D	Wrapped with cylindrical wire	4500–71 000	0.0062	1	0
E	Metal powder deposit	80 000–8700 000	0.079	0.92	0

(iii) the kinematic viscosity and diffusion coefficient which, in turn, depend upon solution composition and temperature
(iv) the constants K and a and hence the nature and extent of surface roughness on the rotating cylinder electrode.

Rough electrodeposits, particularly metal powders, have been shown to enhance reactor performance by virtue of both increased frictional forces at the cathode surface (due to improved micro-turbulence) and a larger active electrode are [28–33]. Such enhanced mass transport [24] combined with the possibility of continuous metal production in powder form (under controlled potential conditions) have been exploited in rotating cylinder electrode reactors which are considered later in this paper.

In the case of deposition of roughened metal deposits, it is difficult to separate the contributions of k_m and A since roughened surfaces enhance mass transport via microturbulence promotion and the true area of the deposit is much greater than the geometric one [27–29]. Two approaches have been suggested [33] to separate k_m and A effects in the expression

$$k_m A = I_L/zFc \tag{8}$$

These are:

(i) Use of predetermined surface roughness obtained by, for example, machining of the RCE, abrasion of the RCE, corrosion/anodic etching or the use of closely conforming wraps of wire or mesh. Geometrical calculations or (preferably) microscopic/profilometric measurements may be used to determine the surface roughness, ϵ, and the area A.
(ii) The determination of active electrode area by (a) measurement of reaction rates under charge transfer controlled conditions (which are insensitive to k_m) or (b) area measurements via impedance spectroscopy, for example.

Method (i) has been used in an extensive study of mass transport controlled copper deposition, from acid sulphate solutions at 'designer-roughened' RCEs by Makanjuola and Gabe [28, 29].

In this study, the Sherwood number was corrected such that the measured current referred to the calculated surface area of the roughened electrode. Figure 4 shows a log–log plot of the modified Sherwood number against the Reynolds number for various roughened RCEs. There are three notable features:

(i) all roughened RCEs show a higher mass transport than hydrodynamically smooth RCEs;
(ii) the degree of mass transport enhancement varies with the type of roughness;
(iii) unlike the smooth RCE, there is a break in the slope of the lines for the roughened RCEs, that is, the mass transport correlation alters above a particular Re value.

In the case of a growing metal deposit, the factors k_m and A will generally show a dependence on solution composition, electrolysis conditions, temperature, time and the type and frequency of scraping in addition to the rotating cylinder electrode size and velocity. The inter-relationship between K, a and U provides a design complication and underlines the need to conduct laboratory and pilot scale studies (which allow K and a to be estimated). This situation for a metal powder deposit on a rotating cylinder electrode, may be contrasted to the case of an hydrodynamically smooth electroplate. In the latter case, the values of K and a have been well-established, at least for small diameter ($D \ll 10$cm) rotating cylinder electrodes [27, 34, 35]. During preliminary sizing exercises, it is useful to have a rough design guide. Based upon the deposition of copper from acid cupric sulphate solutions in a number of Eco-Cell rotating

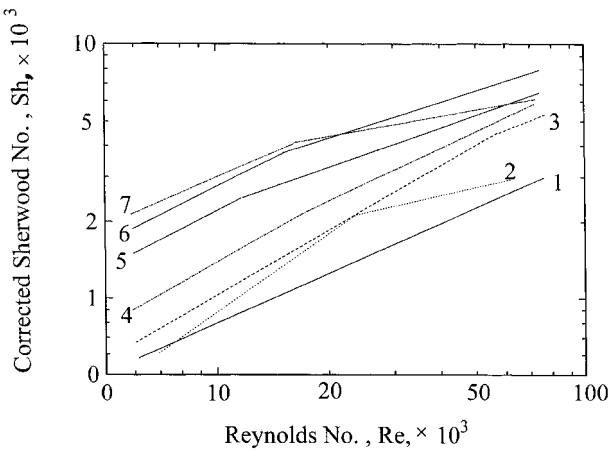

Fig. 4. Enhancement by roughness. Mass transfer correlations (Sh/Re) for several types of roughness using acid copper deposition after Makanjuola and Gabe [10]. Legend: (1) smooth cylinder, (2) longitudinal 'v' groove, (3) circumferential 'v' grooves, (4) pyramidal knurling, (5) wire wound cylinders, (6) weave screen (fine) and (7) weave screen (coarser).

cylinder electrode reactors Holland [36, 37] has suggested that $K = 0.079$ and $a = 0.92$. It should be realized however, that the value of the velocity exponent (a) varies for different reactors; the assumption of $K = 0.079$ is rather arbitrary, being based upon the early studies of the smooth rotating cylinder electrode [25, 26]. Accepting these values, Equation 6 which refers to a metal powder deposit, becomes

$$K_m A = 0.079\pi\ lU^{0.92} d^{0.92} v^{-0.564} D^{0.644} \quad (9)$$

In the case of a hydrodynamically smooth rotating cylinder electrode, a = 0.74 [33, 34] and the analogous relationship is:

$$k_m A = 0.079\pi\ lU^{0.74} d^{0.74} v^{-0.384} D^{0.644} \quad (10)$$

The degree of enhancement for a metal powder deposit with respect to a smooth rotating cylinder electrode may be calculated if Equation 9 is divided by Equation 10:

$$\gamma = U^{0.18}\ d^{0.18} v^{-0.18} \quad (11)$$

or, as a function of the Reynolds number,

$$\gamma = (Re)^{0.18} \quad (12)$$

The result of such calculations is shown in Fig. 5 where γ is seen to markedly depend upon the diameter and the peripheral velocity. In practice, the velocity exponent, a, and the factor, K, depend upon the process conditions, as previously mentioned. Additionally, the development of a roughened metal powder deposit always shows a degree of randomness with regard to the effective $(k_m A)$ value [30, 34, 35].

Figure 5 illustrates two important features: (i) that the performance of metal powder deposits is always superior to that of a smooth rotating cylinder electrode (indeed the latter is not usually economically viable except for precious metals), and (ii) that the enhancement becomes larger at higher velocities. This enables the rotation speed of larger rotating cylinder electrodes to be kept within a reasonable range and at much lower values than laboratory devices.

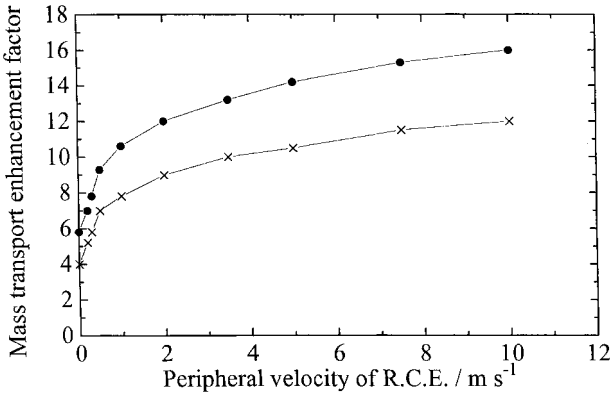

Fig. 5. Idealised mass transport enhancement factors, γ, as a function of peripheral velocity expressing the ratio of $k_m A$ for a metal powder deposit compared to a smooth surface according to Equation 11 assuming $d = 1$, $v = 1 \times 10^{-10}\ m^2\ s^{-1}$, $D = 5 \times 10^{-10}\ m^2\ s^{-1}$. Legend: (●) $d = 10$ cm; (x) $d = 50$ cm.

The rotation speed is governed by the relationship:

$$\omega = U/d \quad (13)$$

and there are various scale-up strategies with respect to the rotation speed. For example, (i) maintain the peripheral velocity at a reasonably high value, (ii) maintain the rotation speed (which presents mechanical problems), and (iii) maintain a constant mass transport coefficient (k_m) enabling a linear scaleup in terms of projected cathode area. In practice, the engineering requirements for a reactor design force many compromises and none of these routes has been followed exactly.

It is possible to combine the high surface area of porous three-dimensional electrodes with the controlled flow conditions offered by a rotating cylinder. Three-dimensional RCEs have particular advantages in laboratory studies of metal ion removal and an early example is the work of Kreysa and Brandner using an RCE comprising a packed bed of carbon granules with radial flow [38]. A more recent example is a study of RCEs which employ a reticulated vitreous carbon (RVC) cylinder [39]. Using copper deposition from acid sulphate solution, mass transport measurements were made via limiting current determination over the rotation speed range 250–2500 rpm. The RVC RCEs had a diameter of 1.0 cm and a length of 1.2 cm and four porosity grades were studied: 10, 30, 60 and 100 ppi (pores per linear inch). The enhanced mass transport, compared to a smooth RCE of the same diameter and length, is shown vs. rotation speed in Fig. 6(a). For the 100 ppi material, enhancement factors of approximately 40 times are achieved. This enhancement can be exploited in the rapid removal of metal ions from a fixed volume, of electrolyte. Figure 6(b) shows the time taken to remove 90% of the original Cu^{2+} level as a function of rotation speed for four grades of RVC, a smooth RCE of the same diameter and length and an RDE of the same diameter. At moderate rotation speeds (1500 rpm), the 100 ppi RVC RCE allows a 200 cm^3 volume of electrolyte to be treated in just over 15 mins, in comparison with some 8 h for the smooth RCE and 30 h for the smooth RDE.

4. RCE reactors

Electrochemical reactors based on the RCE have particularly found use in metal ion removal from dilute aqueous solutions, where the metal can be deposited on the surface of an inner rotating cathode in turbulent electrolyte flow. The enhanced mass transport to such RCE cathodes has already been considered and a number of industrial devices have utilised this (and related) technology. Examples include:

(i) the Eco-Cell [36, 37] and the Eco-Cascade cell [40]
(ii) the MVH cell [41]
(iii) the Turbocel [42]

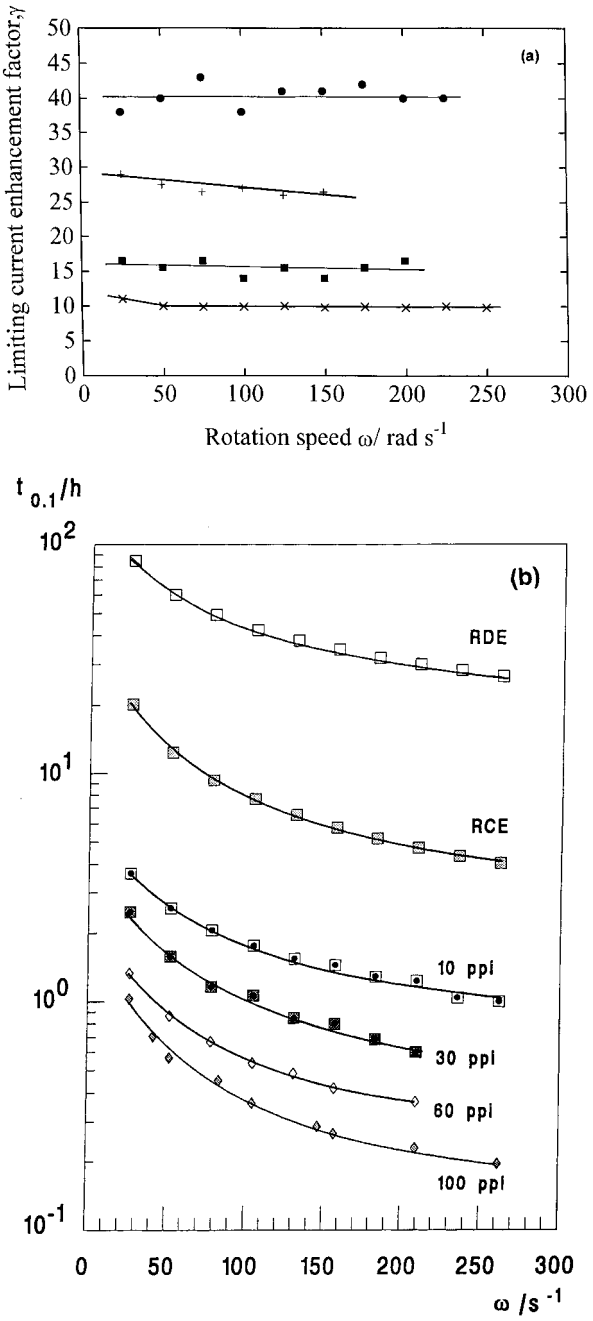

Fig. 6. Mass transfer performance of RVC RCEs. (a) Plot of the limiting current enhancement factor, γ, against rotation speed for four grades of rotating RVC cylinder electrode. Legend: (x)10ppi, (◆)30 ppi, (+) 60ppi and (●)100 ppi. $\gamma = 1$ corresponds to the limiting current at a smooth RCE of the same overall volume as the RVC cylinder. (b) Semilogarithmic plot of time for 90% removal against rotation speed for the four grades of rotating RVC cylinder electrode. Legend: (□)10 ppi, (□)30 ppi, (◇)60 ppi and (◆)100 ppi. Also shown are plots for a smooth RDE of the same diameter and a smooth RCE of the same diameter and length. The solid and broken lines show the predicted performance for a smooth RDE having the same diameter and a smooth RCE having the same diameter and length.

(iv) a cell from Enthone–OMI [43]
(v) a rotating cathode band cell from Heraeus Elektrochemie GmbH [44].

The design and application of RCE reactors in metal ion removal have been extensively reviewed [31, 45, 46] and only selected details will be considered here. Important features of the RCE include the following:

(i) The peripheral velocity, U, normally lies in the range 0.6–20 m s^{-1}, giving rise to turbulent flow conditions around the inner RCE cathode.
(ii) The potential and current distributions are uniform and are time-averaged by rotation, providing a uniform reaction rate over the cathode and facilitating controlled potential separation of metals.
(iii) The mass transport rate is high and can be enhanced via deposition of a roughened (flake or powder) deposit acting as a microturbulence promoter.
(iv) Depending on the reactor geometry and the operating conditions (particularly the cathode potential) metal may be deposited in a variety of forms, ranging from strippable foil through to loosely adherent powder.

Application areas for RCE technology have included metal finishing wastes [32], purification of plating baths [47, 48], hydrometallurgical extraction [49–52], precious metal refining [53], photographic silver removal [54–59] and processing of fissionable materials from spent reactor fuel [63].

An extensive review [45] has considered the diversity of size, scale and design for RCE reactors. Table 3 lists details of ten reactors which have been used for the removal of metal (in powder form) from dilute metal ion solutions. The examples chosen are taken from over twenty rotating cylinder electrode reactors which have provided design and operational experience over a ten year period. The reactor designs are summarised schematically in Fig. 7 and represent a range of laboratory, pilot-scale, and full industrial scale devices. In practice, the size and scale of rotating cylinder electrodes has been much wider than Table 3 suggests. The authors have experienced commercial designs which include a double-sided, 1.2 m diameter rotating cylinder electrode (projected area 2.5 m^2), rotating at 360 rpm. The schematic construction and operation of a divided, concentric RCE cell for metal ion removal is shown in Fig. 8.

In terms of their intended use, the reactors in Table 3 fall into three categories. The laboratory reactors A, B and C were developed as versatile testbeds for feasibility studies. Model A has mainly been used for precious metal removal. Model B was originally designed to study mass transport to roughened (Cu) deposits and controlled potential separation. Recently, it has been rebuilt to study controlled roughness rotating cylinder electrode surfaces and rotating cone electrodes. Model C has been widely used for feasibility trials on industrial process liquors. The flow-through pilot plant reactors D, E, F and G were constructed to provide information on scale up and process operation, including scraper design, manifold positioning, seal and bearing design and product extraction. The mini pilot plant, D has mainly been used for copper, cadmium and cobalt extraction. Models E, F and G have all seen extensive use for copper removal while model E has been used

Table 3. Details of selected single catholyte compartment RCE reactors [8]

Model	*Model type*	*Nominal current rating I*/A	*RCE details*					*Overall space occupied by reactor* /m^3
			Diameter d/m	*Length l*/m	*Projected area A*/m^2	*Rotation speed* /rpm	*Peripheral velocity U*/m s^{-1}	
A	Laboratory beaker cell	< 10	0.050	0.051	0.8000	< 1000	< 2.6	0.001
B	Laboratory bench rig	< 10	0.063	< 0.06	< 0.0040	< 1000	< 3.3	0.025
C	Laboratory test rig	< 100		0.085	0.0200	< 1250	< 6.0	0.050
D	Mini pilot plant	100	0.10	0.062	0.0200	500 to 1500	2.5 to 8.5	0.008
E	Pilot plant	500	0.23	0.23	0.163	500	6.0	0.076
F	Skid-mounted pilot plant	500	0.25	0.25	0.20	240 to 750	3.1 or 9.7	0.060
G	Large pilot plant	2000	0.45	0.41	0.57	460	11.1	0.20
H	Full scale commercial	250	0.45	0.45	0.63	415	9.8	1.4
I	Full scale commercial	5000	0.74	0.74	1.72	406	15.6	2
J	Prototype commercial	40	0.11	10.2	0.0360	1050	6.2	0.090

to investigate cadmium extraction from a concentrated zinc calcine liquor. Models H and I were purpose-built to suit applications involving silver recovery from phthalocyanine effluent, respectively. Model J has been described elsewhere [59] as a prototype system for silver removal from X-ray film fixer liquors. It is interesting to note that the peripheral velocity was normally in the approximate range $1 < U/\mathrm{m\,s^{-1}} < 10$ while the (maximum) rotation speed is decreased for the larger rotating cylinder electrodes. The aspect ratio (d/l) has varied in the approximate range $0.1 < d/l < 2$ [32, 74] but the usual range is much smaller for industrial devices, that is, $0.9 < d/l < 1.6$, as indicated in Table 3.

The fractional conversion per pass in a single catholyte compartment reactor is usually limited to approximately 0.5 [59, 74]. To obtain high overall conversions in a single pass, cascade reactors have been developed [50, 51, 65] by subdividing a long rotating cylinder electrode reactor using baffle plates in the catholyte. Current and potential distribution are critical in these devices [65, 74]. Table 4 summa-

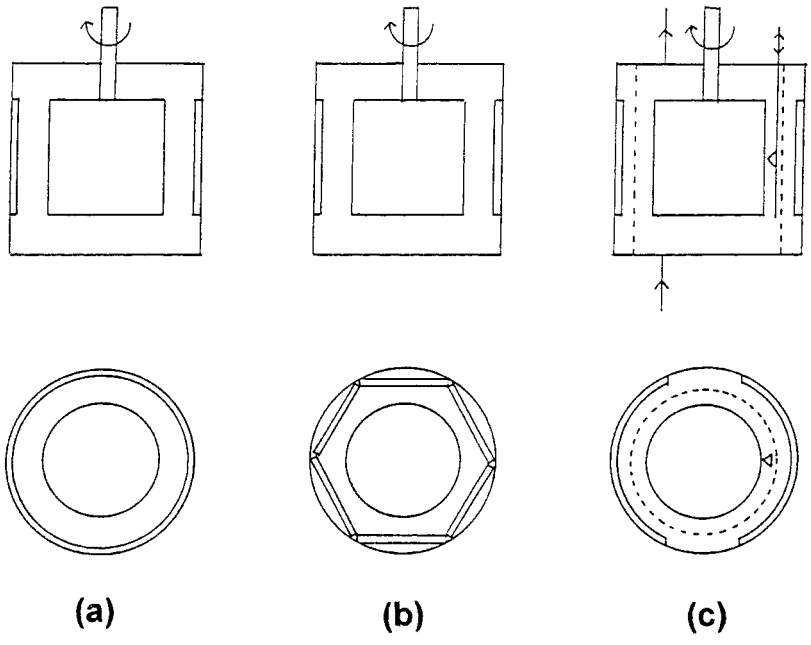

Fig. 7. Designs for concentric RCE reactors involving metal deposition at the inner cathode. (a) Fully concentric undivided cell (idealized); (b) undivided cell using a hexagonal arrangement of anode plates (commonly used in photographic silver recovery); (c) divided cell in which a scraper is used to dislodge metal powder deposits (as in the Eco-cell).

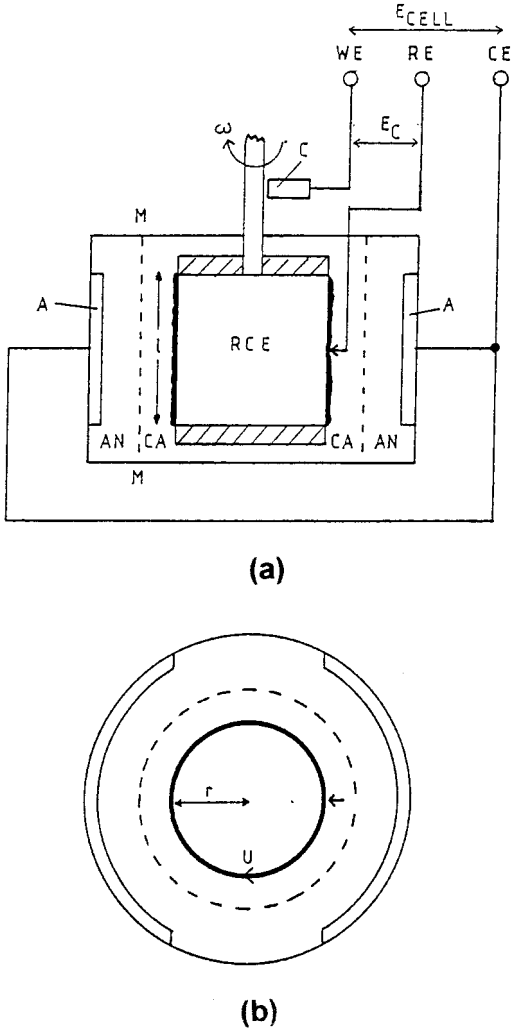

Fig. 8. Principles of electrical control and measurement in a RCE reactor: (a) sectional view and (b) plan view. Key: (A) anode, (C) brush contact to cathode, (WE) working electrode, (CE) counter electrode, (RE) reference electrode, (M) membrane cell divider, (CA) catholyte, (AN) anolyte, (l) active length of RCE, (U) peripheral velocity, ($\overline{\omega}$) rotational velocity, (P) insulating end caps, (RE) probe, (E_c) cathode potential, (E_{cell}) cell voltage.

rizes the essential characteristics of five models of cascade rotating cylinder electrode reactor. These devices were mainly constructed as prototype reactors, extensive test work having been carried out using acid cupric sulphate electrolytes on models I, II and III. Laboratory studies using model I helped to provide a design basis for a commercial cascade reactor (model II) which is used as a secondary unit after a single rotating cylinder electrode [40]. Model III involved a radical change in design but the performance was problematic [40, 45]. Model IV was purpose-built as a commercial reactor to remove silver from photographic fixer liquors [55]. In fact, it was designed rapidly on the basis of data from a small single rotating cylinder electrode (model A in Table 2) and was installed as a secondary unit in a process loop which used reactor H as the primary device. Model IV has recently changed its aspect and has become a test facility. The last model listed (V) was constructed to critically examine the degree of

Table 4. Summary of the Charateristics of Cascade Rotating Cylinder Electrode Reactors for Metal Ion Removal.

Model type	*Metal removed*	*Solution treated*	*Nominal current* /A	*Number, n, of catholyte compartments*	*Volumetric flowrate, Q* /$m^3 h^{-1}$	*RCE diameter, d* /m	*RCE total length, l* /m	*RCE area in each catholyte compartment* /m^2	*Rotation speed, ω* /rev min^{-1}	*Peripheral velocity, U* /m s^{-1}	*Aspect*
Laboratory pilot plant (I)	Cu	Acid sulphate	100	10	0.36	0.076	1.00	0.0215	2000	8.0	Horizontal
Full scale Commercial (II)	Cu	Copper phthalocyanine effluent	1000	12	8	0.324	2.88	0.204	860	14.6	Horizontal
Development/ pilot plant (III)	Cu	Acid sulphate	500	6	1.8–3.6	0.306	1.00	0.139	730	11.7	Vertical
Full scale commercial IV	Ag	Photographic fixer	100	10	0.1	0.216	1.07	0.067	780	8.8	Vertical, (later horizontal)
Laboratory test facility (V)	Cu Ag	Acid sulphate Photographic fixer	20	1–10	0.12–1.5	0.050	1.02	0.016–0.160	60–750	0.15–2.0	Vertical or horizontal

flow bypassing and the potential distribution under a wide range of flow conditions, following shortcomings with earlier models.

In laboratory studies, rigorous control of the cathode potential may be attained using the three-electrode arrangement shown in Fig. 8 and a potentiostat. In pilot and full scale operations, it is usually more difficult to precisely control parameters which affect the limiting current, including cathode surface state, electrolyte composition, volumetric flowrate and cathode potential. For example, high current reactors may have a large *IR* drop associated with measurement of the cathode potential. This can arise from several sources including voltage drops across the power brush contact, along the rotating cylinder electrode shaft and cathode construction and between the reference electrode probe and the metal powder deposit. These effects may be minimized. For example, the potential difference across the power brush/slip ring assembly may be bypassed by the use of an auxiliary potential sensing contact [48, 58, 59, 75]. The extent of such *IR* drop may vary with time due to variable contact surfaces and may be appreciable in pilot scale reactors (see Fig. 9).

Another practical problem in pilot-scale reactors is the loss of current efficiency due to the presence of dissolved oxygen (from aeration or anodically evolved oxygen). A series of recent papers has considered the modelling of RCE reactors in the presence of dissolved oxygen [60–62]. The authors have derived expressions relating dissolved oxygen concentration to geometrical and operational characteristics relevant to metal ion removal in the following cases:

(i) Oxygen reduction from 1 M KOH in an undivided reactor [60].
(ii) Oxygen reduction in a reactor divided by an ion exchange membrane [61].
(iii) Cupric ion removal in an undivided reactor in the presence of dissolved oxygen and metal cation contaminants in a pH 4 mine tailing liquor [62].

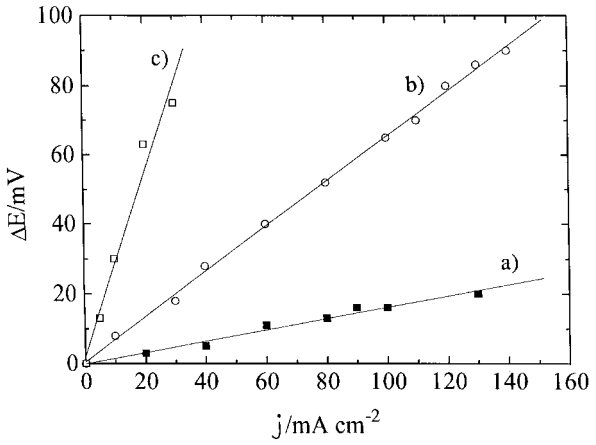

Fig. 9. Potential drop over RCE electrode systems as a function of current, showing ohmic losses (a) potential drop between the RCE potential sensing brush and the cathode power brush for laboratory reactor model B; (b) potential drop between the RCE shaft and the cathode power brush for pilot scale reactor model E; (c) potential drop across the ends of a double-shafted cascade reactor model C.

The most detailed consideration of quantitative RCE reactor performance has appeared in a series of papers on a pilot scale reactor ($d = 24.8$ cm, $A = 198\ \text{cm}^2, \omega = 750$ rpm) used to recover copper from 0.5 M H_2SO_4 at 35 °C [49–51]. Single pass [49] and batch recycle [50] operation has been considered. Figure 10 shows data from these studies. In the batch recycle mode, an inlet cupric ion concentration of 460 ppm is reduced to 7 ppm with time, a constant fractional conversion being achieved (as evidenced by the parallel decay line for the outlet concentration). Under potentiostatic control, the current also decays with time, although the current efficiency for cupric ion removal still falls with time (due to hydrogen evolution and oxygen reduction as secondary reactions). Walsh [51] has critically considered the determination of mass transport data from RCE reactors used to remove cupric ion and has shown that the reactor closely conforms to a CSTR model. It was also shown that, at high values of fractional conversion per pass, it was important to adopt a batch recycle model rather than a simple batch model [51].

The enhancement of mass transport in a concentric RCE reactor with axial flow by plastic mesh turbulence promoters has been studied by Eklund and Simonsson [70]. In comparison to an unpromoted annulus with a smooth rotating cylinder, enhancement factors of up to six times were found.

In the case of silver recovery from photographic fixer solutions, potentiostatic control of an RCE cathode can be used to provide high current efficiency and to facilitate silver powder removal from the reactor via scraping. Following extensive laboratory and pilot scale studies by Walsh *et al.*, the Ilford Co. developed patented technology based on this work [71].

The performance of six electrochemical cells for silver ion removal: a plate-in-tank cell, a pumped tank cell, a rotating cylinder electrode cell, a Chemelec cell and a DEM cell containing graphite granules or carbon felt has been considered [63]. Under the experimental conditions, the Chemelec cell and the rotating cylinder cell produced similar current efficiencies, although the lack of potential control resulted in very low values, typically 0.6–1.7% at an operating current density of 150 A m^{-2} and silver ions in the range 13–21 ppm. To achieve residual silver levels <10 ppm, the use of three-dimensional, porous carbon cathodes was recommended. The second paper examined the electrolytic regeneration of bleach fix solutions by the anodic oxidation of ferrocyanide at 30 °C in a divided cylindrical cell stirred by a central rotating cylindrical anode [64]. A voltammetric study indicated that the anode reactions include oxidation of ferrocyanide to ferricyanide as well as bromine and oxygen evolution at more positive potentials. Under the experimental conditions, using 350 cm^3 of an electrolyte containing

$20\,g\,dm^{-3}$ potassium ferrocyanide, 5–$50\,g\,dm^{-3}$ potassium ferricyanide and $25\,g\,dm^{-3}$ potassium bromide, the maximum anodic current efficiency for ferrocyanide oxidation was 85%. The preferred conditions were an anode potential of 0.8V vs SCE and a cell with a graphite rod anode (diam. 2.7cm, length 10cm), rotating at 400rpm. The current efficiency fell markedly at higher current densities and at lower ferrocyanide concentrations. In comparison to the use of ozone or persulphate, the electrochemical route to regeneration of the ferricyanide bleach fixer solution is more convenient and avoids the use of corrosive chemicals. A vertical, stainless steel RCE ($d = 5.0\,cm$, $A = 160\,cm^2$, $\omega = 10-200\,rpm$) has been used to continuously strip copper foil from a concentrated solution containing $150\,g\,dm^{-3}$ $CuSO_4.5H_2O$ and $50\,g\,dm^{-3}$ H_2SO_4 at 40 °C [65]. This technology has been developed to directly electrorefine cemented copper anode material [66] in a diaphragm cell; 99.98 wt % Cu deposits could be obtained as 3 mm thick sheets at a current density of $5\,A\,dm^{-2}$. The adverse affects of As(v) and Fe(II) ions on the energy and current efficiency for copper electrowinning from acid sulphate solutions at a rotating drum cathode have also been considered [70].

The anodic generation of oxidants such as Ag(II), Co(III), and Fe(III) at an inert (Au or Pt) RCE has been described [67]. The divided RCE reactor geometry was chosen to enable a small batch apparatus to be used which mimicked mass transport conditions in a flow through pilot plant. The RCE ($d = 1.2\,cm$, $\omega = 1500\,rpm$) was operated at 25–60% of the limiting current for oxidant (redox mediator) generation and was used to destroy organic wastes. The authors discuss mathematical models to describe the interaction between the redox mediator and the organic.

The 'RCE-in tank' geometry has been extensively used for organic electrosynthesis, particularly at the Central Electrochemical Research Institute, Karaikudi in India. A comprehensive review of organic oxidations and reductions using the RCE has been provided [68] which also describes the construction of laboratory cells and those operated at 500–3000 A, for example, for calcium gluconate and benzidine synthesis.

More recent examples of electroorganic synthesis at rotating cylinders have included:

(i) Catalytic alkylation of phenols [73] (including salicylic acid methyl ester and *p*-cresol) with isobutene, where an inert, rotating PTFE cylinder reactor has been shown to be superior to agitated vessels for slow multiphase reactions.
(ii) Cathodic reduction of carbonyl compounds in acid media to form hydrodimeric and hydromonomeric productions, for example, reduction of *p*-methylbenzaldehyde at a lead RCE ($d = 0.5\,cm$, $l = 5\,cm$, $\omega = 250$–$1500\,rpm$) in a divided, 'beaker-type' cell [74]. The product selectivity could be controlled via selection of the rotation speed.
(iii) Reduction of methyl cinnamate to various hydrodimeric products at a copper RCE ($d = 0.6\,cm$, $l = 5\,cm$) where a high rotation speed is essential to optimize the current efficiency when using a high current density [75].

The use of an RCE reactor for continuous electrophoretic separation of proteins has been described [53]. In the Biostream Process developed at Harwell, UK, electrophoresis takes place in an annulus (typically 3 mm wide) between the inner and outer cylinders of the separator. A buffer electrolyte (the carrier solution) flows upward through the annulus. Stable laminar flow of the carrier solution is maintained by rotation of the outer cylinder (rotor). This overcomes the problem of convective turbulence which would otherwise be caused by resistive heating. The inner cylinder (stator) is held stationary. Concentric with the annulus are compartments formed in the rotor and stator which contain the electrodes (stainless steel) and their electrolytes. These are isolated from the carrier solution by dialysis membranes of regenerated cellulose which are supported on inert porous tubes. An electric field is applied across the electrodes, typically 30 V at 60 A. The mixture to be fractionated (the migrant) is injected into the carrier solution through a thin slot around the base of the stator. The components of the migrant mixture separate under the force of the electric field by moving at different rates towards the outer wall of the annulus. They thus form concentric bands within the annulus. Applications of the device include fractionation of blood plasma, isolation of enzymes from muscle extracts and the separation and concentration of platelet cells from red blood.

5. Voltammetry

One aim of voltammetric analysis is to utilize limiting (diffusion) current values, determined from potential vs current relationships, to measure certain solution characteristics – notably ionic concentrations and ionic diffusion coefficients. For this purpose a well-defined hydrodynamic condition is necessary, usually one in which forced convection is not only stable but sufficient to overcome free convection variability or uncertainty. Both the RDE and RCE can meet this criterion, the former in laminar flow and the latter in turbulent flow. Historically, the RDE has been extensively used largely because of its early establishment by Levich's pioneering work on fluid flow and mass transport.

The earliest examples, which have been mentioned in the first review [12], often employed a simple rod cathode rotated without especial attention to the precise hydrodynamic conditions. No advantage over the RDE was appreciated until the need to separate mixed metals in solution was identified, for which the additional requirement of an equipotential surface together with sufficient surface area was recognized. Johansson [76] utilized the separating ability, to-

gether with coulometric measurement, to analyse chromatographic fractions of silver and copper in particular. The ability to selectively electrodeposit trace amounts of metal in solution was used by Vaaler [48] to successfully purify nickel plating solutions of more base metals especially iron and zinc but also to eliminate copper at low concentrations with the help of increased agitation and lower current densities. A further extension of this methodology was used by Walsh and Gabe [32] to separate gold, silver and copper as part of an effluent treatment exercise for which an additional factor of differential cyanide complexing existed.

While many voltammetric analysis procedures rely on the proportionality $i_L \propto C$, mass transfer analysis requires knowledge of the diffusion coefficient, D of the electroactive species and the RCE provides a means of measuring its value. The RDE is a standard technique for such determinations but the RCE may equally well be employed. Burgman and Sides [77] have used both methods in fused salt cryolite melts and provided detailed analyses of the various ion species involved whose importance for the Hall–Heroult process has long been uncertain.

Classical analytical use to determine concentration values has been associated with other features for electroplating solutions by Vanhumbeeck and Doncker [78, 79] who noted in particular the influence of additives in solution and the possibility of assessing deposit quality as a function of current density. Using the RCE they were able to establish deposit morphology diagrams for high speed palladium solutions for the first time.

A number of voltammetric methods have been proposed for the measurement of true surface areas of rough electrodes; these all exploit supposed constant or stable convection regimes and by measuring i_L for surfaces of different roughness enable good indications of relative and absolute areas to be measured and hence a measure of roughness. Puippe [42, 80] has recognized the time dependence of such an approach and used a pulsing technique; Gabe and Makanjuola [11, 81] utilized a potential-step technique to determine i_L, then used it to compare relative roughness which could be calibrated using surface mensuration analysis. The technique has been commercialized as the DIN instrument which is used for irregularly shaped electrode surfaces (e.g., jewellery to be gold plated) in order to define the optimum current requirement for a bright finish.

The RCE can in principle be used as a microelectrode and a number of seminal proposals have been made [82, 83]. A particularly interesting suggestion is to develop an *in situ* rotating pH electrode as disc or cylinder to measure pH at a surface where hydroxide precipitation or gas evolution is occurring [84]. Some further evaluation is required for these proposals.

The controlled electrolyte flow and relatively large/renewable surface of an RCE can be advantageous in studies of adsorption at electrodes. For example,

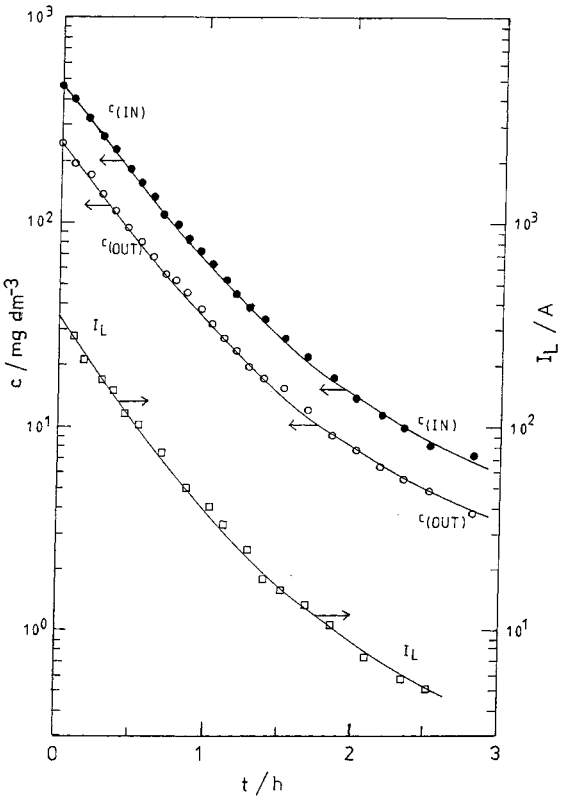

Fig. 10. Copper concentration and current decay in the batch recirculation mode, Reactor model F. Conditions: 0.5 M H_2SO_4 at 35 °C, $Q = 25\,dm^3\,min^{-1}$, $V_T = 436\,dm^3$, $\overline{\omega} = 750$ rpm, $E = -0.430$ to -0.500 V vs SCE.

surface-enhanced Raman spectroscopy studies have been carried out at an RCE [85].

It is not always appreciated that mechanistic and kinetic studies can be readily carried out at an RCE (rather than, say an RDE). Indeed, the relatively large current at the RCE can provide higher sensitivity towards reactants. (Although care must be taken to avoid the problem of uncompensated IR drop in the electrolyte gap between the RCE working electrode and the reference electrode.) Morrison *et al.* [86] have shown that accurate measurements of the charge transfer rate constant for the Fe^{3+}/Fe^{2+} couple in acid sulphate solution can be achieved at a platinum RCE surface.

The complementary characteristics of the RDE and RCE have been noted in the literature [23, 45]. The flat RDE surface tends to be easier to prepare (particularly if a low degree of surface roughness is required via polishing) and the electrode is well accepted for charge transfer studies [87, 88]. On the other hand, the RCE should be a preferred electrode for turbulent flow studies involving morphological changes and mass transport controlled depletion of reactants. It is interesting to note that studies of the effect of organic additives on copper deposition have used both the RDE and RCE geometries [89, 90]. Charge transfer and mass transfer kinetics were established via Tafel plots at a copper RDE [89] whereas investigations of metal ion removal under mass transport control involved a copper RCE [90].

In comparison to rotating disc, hemisphere, cone or wire electrodes, the RCE can provide a relatively high ratio of electrode area per unit electrolyte volume. This can be exploited in controlled potential coulometry studies where the experimental time for exhaustive electrolysis can be kept short, particularly if the RCE is fabricated from a porous, three-dimensional material such as reticulated vitreous carbon, RVC [91, 92].

Rotating microelectrodes give rise to a limiting current density which increases as the characteristic size (diameter or width of the electrode is reduced due to the increasing importance of the non-perpendicular component of diffusion towards the electrode surface. The micro rotating cylindrical strip electrode is a useful geometry; the vertical-line electrode constitutes a microelectrode in one (width) dimension perpendicular to the direction of electrode motion, but is infinitely large in its other (length) dimension. This results in a reasonably high surface area (typically 0.005–0.05 cm^2) which enables current to be easily measured without using specialized low current amplifiers. Workers at Tel-Aviv University [93] have described an RCE consisting of three strips of gold (width: 20, 90 and 200 μm length 3.5 cm embedded longitudinally in a cylindrical glass sheath 18 mm diameter and 50 mm length. Using the oxidation of 5 μM ferrocyanide in 0.1 M KCl at 25 °C as a test reaction, well-defined limiting current plateau were observed over the rotational speed range 100–6400 rpm (although baffles were needed to prevent solution vortexing above 2500 rpm).

The results illustrate several important features of microline electrode RCEs:

(i) In comparison to a macro RCE, mass transport is enhanced by up to 12 times, the effect being most pronounced for the thinnest (20μ m) electrode at low rotation speed (400rpm) as shown in Fig. 11(a).
(ii) The line microelectrodes at 6400rpm gave mass transport rates equivalent to those calculated for an RDE at 6×10^6 rpm.
(iii) For the 20 μm wide electrode, the mass transport enhancement factor was 30 compared to a rotating disc at 6400 rpm (Fig. 11(b)). Decreasing the width of the microelectrode to 1 μm results in a mass transport enhancement factor of approximately 75 at 6000 rpm in comparison to an RDE [94].

Rotating cylinder electrodes can be designed to combine the advantages of a microelectrode [96] and a macroelectrode into a single electrode assembly (Fig. 12). Walsh [94] has considered two examples: the μ-PERCE (micropoint electrode in a rotating cylinder electrode) and the μ-LERCE (microline electrode in a rotating cylinder electrode). The former consists of a circular micro disc electrode mounted flush with (and insulated from) the RCE surface. The latter utilises a micro band electrode running the length of the RCE. Typically the microelectrodes have a diameter or width of 5–10 μm.

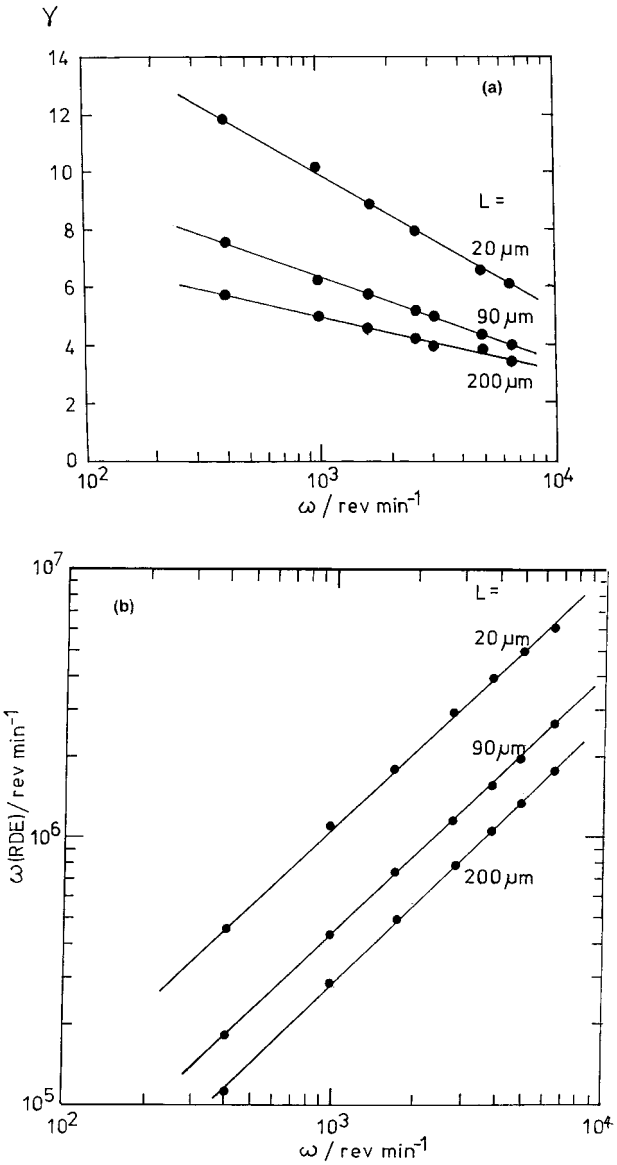

Fig. 11. Mass transport to rotating vertical line microelectrodes: (a) mass transport enhancement factor as a function of rotational speed, the vertical axis showing the ratio of limiting current density at the rotating vertical line microelectrode (L = length) compared to a macro RCE; (b) apparent rotation speed of a RDE as a function of applied rotation speed of a rotating vertical line microelectrode for the same current density.

6. Electrodeposition

6.1. *Electrodeposition of materials*

The RCE geometry has been widely used in laboratory studies and practical, larger scale applications involving electrodeposition. The majority of studies have concerned metal ion removal from dilute aqueous solutions for environmental treatment [13, 31, 96, 97] (see also the 's' section on RCE reactors). However, the area of process control in metal electrodeposition has attracted interest [23, 98]. In the case of commercial, high-speed electroplating three geometries are currently employed which involve strip

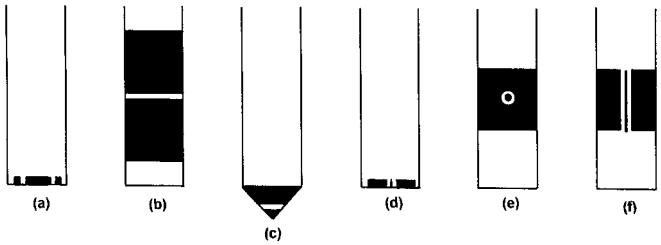

Fig. 12. Combination rotating electrodes mounted on a common shaft. Key: (a) rotating ring disc electrode, (b) double rotating cylinder electrode, (c) double rotating cone electrode, (d) micropoint electrode in a RDE, (e) micropoint electrode in a RCE and (f) microline electrode in a RCE.

movement (in serpentine or horizontal cells), reel to reel wire or strip movement or radial cells (which are routinely used for the electroforming of foils). These geometries can be simulated by a laboratory or pilot scale RCE. The use of a particular RCE peripheral velocity to simulate equivalent electrolyte or linear electrode movement has long been realized [99, 100].

The morphology of metal deposits can be quantitatively studied as a function of current density (i) and rotation speed (ω) of an RCE. Resultant i against ω plots provide useful morphology diagrams which describe the zones for particular types of electrocrystallization. Examples of the use of the RCE to derive morphology diagrams [101] include alkaline zinc [102], acid zinc [103], cyanide gold [104], palladium–nickel [79] and zinc–nickel [105]. Figure 13 shows a morphology diagram for Zn–Ni deposition [106].

Mass transport rates in zinc electrowinning from an acid sulphate solution have been determined by Cathro [107] at an RCE of 15.8 mm diameter, 10.0 mm length with a 0.25–4.0 m s^{-1} peripheral velocity. The k_m values determined were higher than values predicted from literature correlations but the discrepancy was attributable to enhancement by hydrogen evolved as a secondary product (although anodically evolved oxygen may also have contributed).

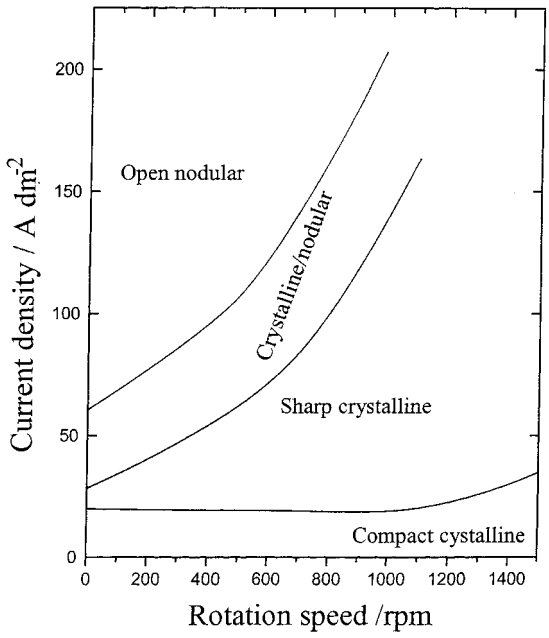

Fig. 13. Electrodeposit morphology diagram for Zn–Ni alloy deposits from an acid solution after Wilcox and Gabe [106].

A number of authors have developed RCE cells having a range of current densities on the RCE cathode via the use of a controlled range of anode–cathode gap at a constant applied current (Figs. 14 and 15). Such devices may be viewed as a progression of the Graham–Pinkerton cell [108]. Examples include:

(i) Studies of primary and secondary current distribution for copper deposits from acid sulphate solutions [109].
(ii) Use of a rotating cone cathode and a static, outer cylindrical anode for copper deposition [110].
(iii) Current density distributions for copper deposition from acid sulphate using an RCE cathode and a flat, inclined anode [111].
(iv) Polypyrrole deposition on an RCE anode with an RCE cathode on the same shaft [112].

Many workers have used an RCE cathode to provide a controlled agitation substrate for metal deposition studies. Examples include:

(i) Studies of the ductility and tensile strength of copper electro deposits onto stainless steel from an acid sulphate bath containing organic additives [113, 114].
(ii) Analysis of organic additives in an acid copper sulphate bath by cyclic voltammetric stripping of copper deposits on an Inconel 600 RCE [115].
(iii) Experimental modelling [116, 117] and studies of roughness development during copper electrodeposition from acid sulphate, relevant to electroforming of several hundred micron deposits at a rate up to 110 μm min^{-1}.
(iv) Electrodeposition of Ni–Zn–P alloys from an ammoniacal chloride solution where the alloy deposition process was found to be controlled by the zinc deposition rate at low temperature but by the nickel deposition rate at higher temperature [118].
(v) Electrodeposition of amorphous Fe–Ni–P alloys onto copper substrate RCE cathodes from a sulphate/acetate/hypophosphite bath [119].

(vi) Production of Ag–Sn [120] and Ni–Sn [121] alloy powders as part of a programme aimed at producing dental alloy and other corrosion resistant materials.
(vii) Electroplating of copper into tubular holes using coaxial rotating screw counter electrodes as part of an investigation into through hole plating [122].
(viii) Anodic deposition of Leclanché battery grade MnO_2 onto a titanium RCE [123].

The commercial realization of electropolymerised conductive films often dictates the use of a continuous production process and several groups have used a rotating cylinder electrode (RCE) for this purpose over the last decade. As in the case of electroforming of metal sheet (or the production of particulate metal), the horizontal RCE is partially immersed, enabling the deposit to be scraped off as a continuous film (or as a powder). For example, the production of polypyrrole on a one-third immersed stainless steel RCE (diameter 1.6cm and length 9.5 cm, rotating at peripheral velocities of 0–8.7 cm s^{-1}) has been reported [124]. The electrolyte used was 0.29 M pyrrole in 0.21 M potassium *p*-toluenesulphate at 20 °C, with a current density of 6 mA cm^{-2}. The importance of fluid flow conditions was evidenced by the physical properties of the films at various linear velocities. At 1.67 cm s^{-1}, a flexible polymer having a conductivity of 25 S cm^{-1} was produced whereas at the much lower speed of 1.67×10^{-4} cm s^{-1}, powdery deposits of 5.5 S cm^{-1} were seen. The use of an ultrasonicated partially immersed RCE for deposition of polyaniline and polypyrrole films onto microporous (carbon-loaded polyurethane) films has also been described by the same group [125].

6.2. *Mechanism of electrodeposition*

The rotating cylinder electrode has several favourable attributes that make it an attractive research tool to aid the interpretation of electrodeposition processes. The low speed laminar to turbulent flow transition effectively means that all but the very slowest rotation rates (typically <50 rpm) will result in a turbulent flow regime. The inherent ability also allows the RCE to simulate high speed electrodeposition processes at a laboratory scale, the RCE having a distinct advantage over the continuous circulation cell (CCC) in terms of smaller scale fabrication and low electrolyte volume requirements.

The experimental utilization of the RCE in this type of investigation has been reported by a relatively small number of investigators. Swathirajan and Mikhail [118] have utilized the RCE as the basic tool with which to examine the electrodeposition of Ni–Zn–P alloys. Investigations were concerned with the measurement of partial polarization currents for alloy constituents and an examination of the rate limiting factors of the electrodeposition process. Further investigations [126] used the RCE to produce coatings on foil substrates for subsequent corrosion testing. Similar work on alloy systems has been carried out by Sturzenegger and Puippe who investigated palladium–silver systems [127]. A copper RCE was utilized as the cathode material, the measurement of alloy composition against rotation speed allowing an analysis of electrodeposition mechanisms of the alloy components to be elucidated. Such an analysis suggested that silver was mass transport controlled and careful measurement of silver limiting currents allowed calculation of silver contents of the Pd–Ag alloys to be predicted. Kalantary *et al.* [128] have used the RCE as a basic laboratory simulative for high current-high agitation processes found in industrial electrogalvanizing and, in this manner, have examined the possibility of producing compositionally modulated zinc–nickel alloy coatings. Foo *et al.* [129] used a similar experimental configuration to examine morphological and mechanistic data for zinc and zinc–manganese electrodeposited coating systems for ferrous substrates.

The RCE has also been utilized as a surface on which to electrochemically deposit metal powders; silver and its alloys have been deposited from ammonical [130] and cyanide containing electrolytes [131]. Stainless steel cylinders or the application of an electrode wiping system allow the metal powder to be readily detached and saved. Again the RCE facilitated itself as a useful analytical tool, proving that silver was mass transport controlled and that for Ag–Sn and Ag–Sn–Cu alloys, tin was activation controlled.

The RCE lends itself as an effective surface on which to perform electroforming operations. In this manner Barkey *et al.* [116, 117] have produced copper electroforms at which the effects of agitation and current density could be evaluated from measurements such as surface profilometry and scanning electron microscopy. The effects of surface roughness on limiting current density were also addressed.

Solution reduction reactions can also be conveniently followed using the RCE. Radwan *et al.* [132] have studied one such reaction, the reduction of Cr(VI) to Cr(III) at a gas-evolving electrode. A lead RCE was used to aid measurement of the reaction rate constant and cathode current efficiency against the rotation speed of the electrode.

Although for most of the electrodeposition studied the RCE has been used in a conventional form, some researchers have modified its geometry or the flow pattern promoted by its rotation. Kelsall and Page [133] have used a rotating split cylinder bielectrode to study the oxidation and reduction of chalcopyrite ($CuFeS_2$). Wilcox and Gabe attempted to increase cell turbulence with the imposition of jetted electrolyte flow onto that produced by an RCE [134], no mass transfer correlation has been offered. Jackson *et al.* [135, 136] have used the RCE to simulate electrolytic tinplate production in the manner suggested earlier by Gabe [23], the theoretical background of which will be discussed later.

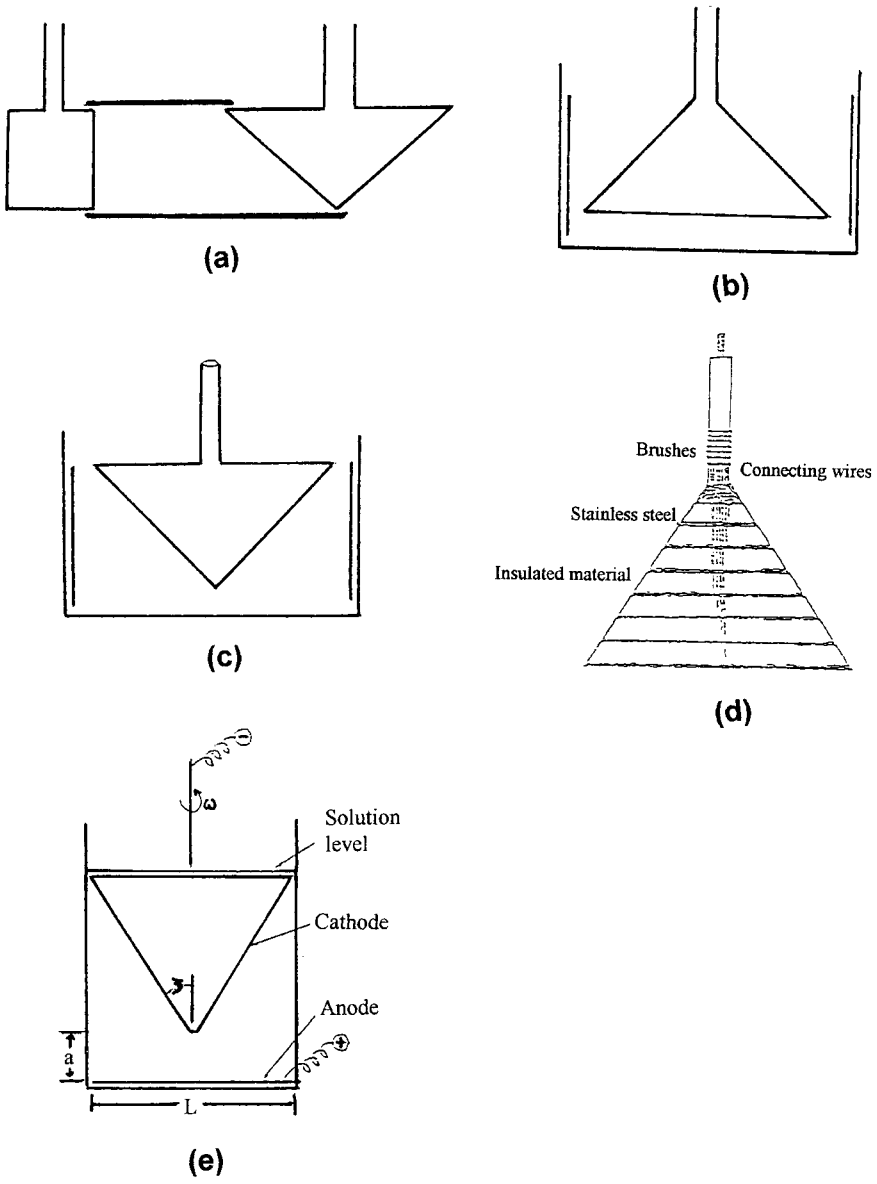

Fig. 14. Agitated current distribution cells using conical geometry. (a), (b) Afshar *et al.* [141]; (c), (d), (e) Afshar *et al.* [141] and Lu[144].

6.3. *Hull cell applications*

Current distribution studies have been made on a number of rotating electrode surfaces. Devaraj *et al.* and Landolt *et al.* [109, 111, 137–139] have investigated the RCE and Reichenbach [140] and Afshar *et al.* [141] the RConE. The specific problem of solution resistance for RCE cells has been studied separately by Bisang and Kreysa [142] who have used the Wagner Number as a criterion for rationalizing solutions of differing conductivity in a model reactor. Prediction of behaviour is best for highly conducting solutions of large Wagner number

$$Wa = \left(\frac{d\eta}{di}\right)\left(\frac{\kappa}{L}\right) \qquad (14)$$

where $d\eta/di$ is the polarization slope, κ is the solution conductivity and L is a characteristic dimension.

The need for such studies exists because the current distribution over cathode surfaces can vary due to a number of reasons associated with resistance or overpotential and electroplating shops need to be able to control in a predictive manner the current density being employed. The effect is summarized below by referring to three types of electrode or cell:

Electrochemical control	Current distribution	Typical cell example
Solution resistance	Primary	Haring-Blum
Activation overpotential	Secondary	Hull
Activation and concentration overpotential	Tertiary	Rotating electrodes

Shortcomings arise due to number of factors, e.g. temperature, agitation, volumetric errors, metal depletion etc., which have been discussed fully elsewhere [110, 143], and a substantial number of variations on these classical designs have been explored [110].

Both RCE and RConE. based designs have a virtue of retaining the Hull cell geometry concept while introducing well-controlled electrode movement, the alternative of solution agitation or pumping being much less satisfactory for quantitative analysis. The design options, or more particularly those employed to date, are illustrated in summary form in Figs 14 and 15 in which several ingenious formats may be noted. The efficacy of any specific design may be defined in terms of (a) a good correlation of current

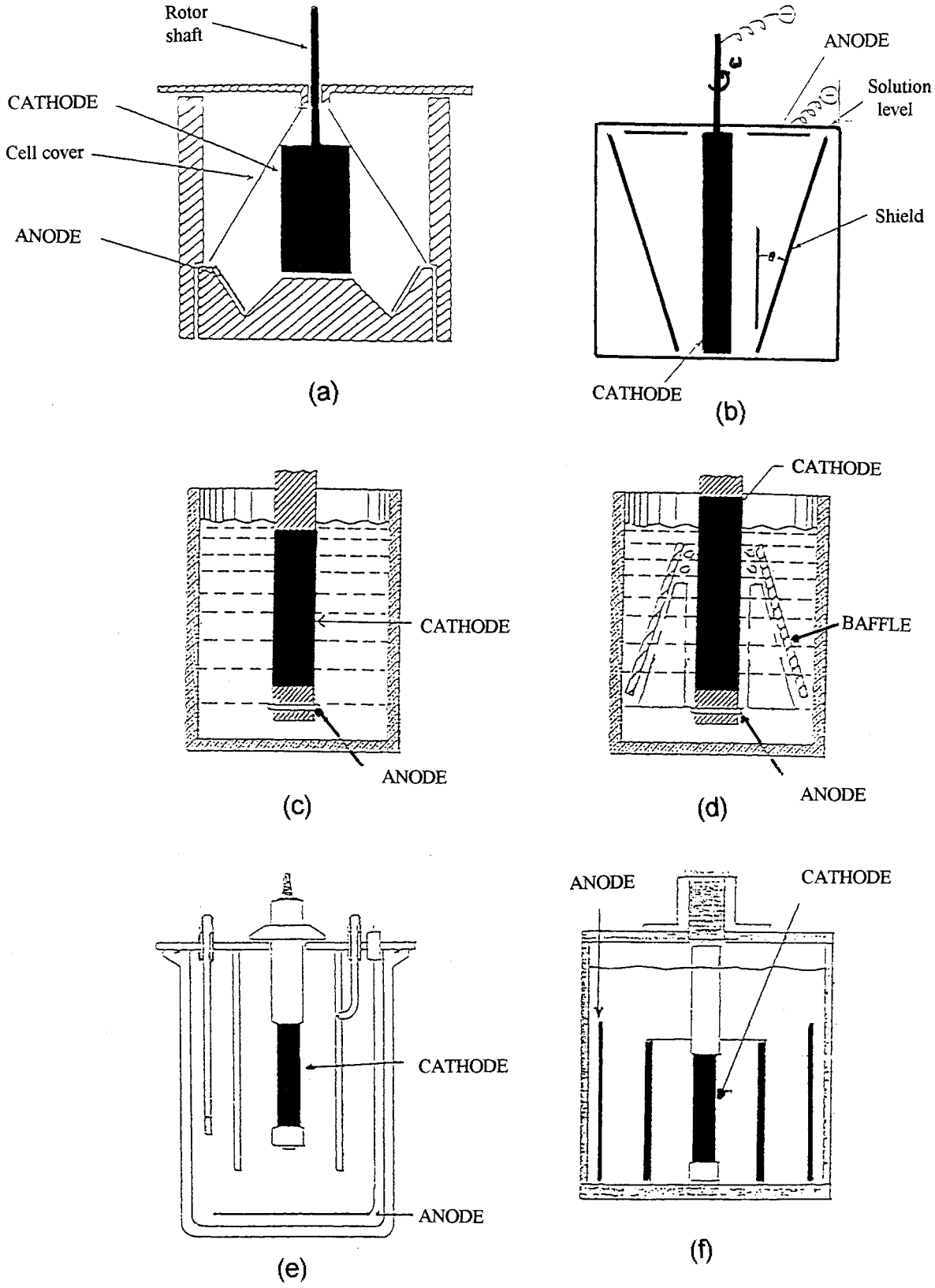

Fig. 15. Agitated current distribution cells using cylindrical geometry. (a) Afshar *et al.* [141]; (b) Lu [144]; (c), (d) Kadija *et al.* [145]; (e), (f) Madore *et al.* [137,138].

density to agitation/rotation value, and (b) practicality in use.

Some relevant correlations are summarized graphically in Fig. 16; the practical utilization for these designs has not yet been established but at the time of writing Landolt *et al.* [109, 111, 137–9] have demonstrated satisfaction most effectively.

7. Corrosion of metals

In the earlier reviews it was pointed out that numerous corrosion or anodic dissolution investigations had made use of the RCE but that they were essentially empirical studies without fundamental design and control of rotation for mass transfer analysis.

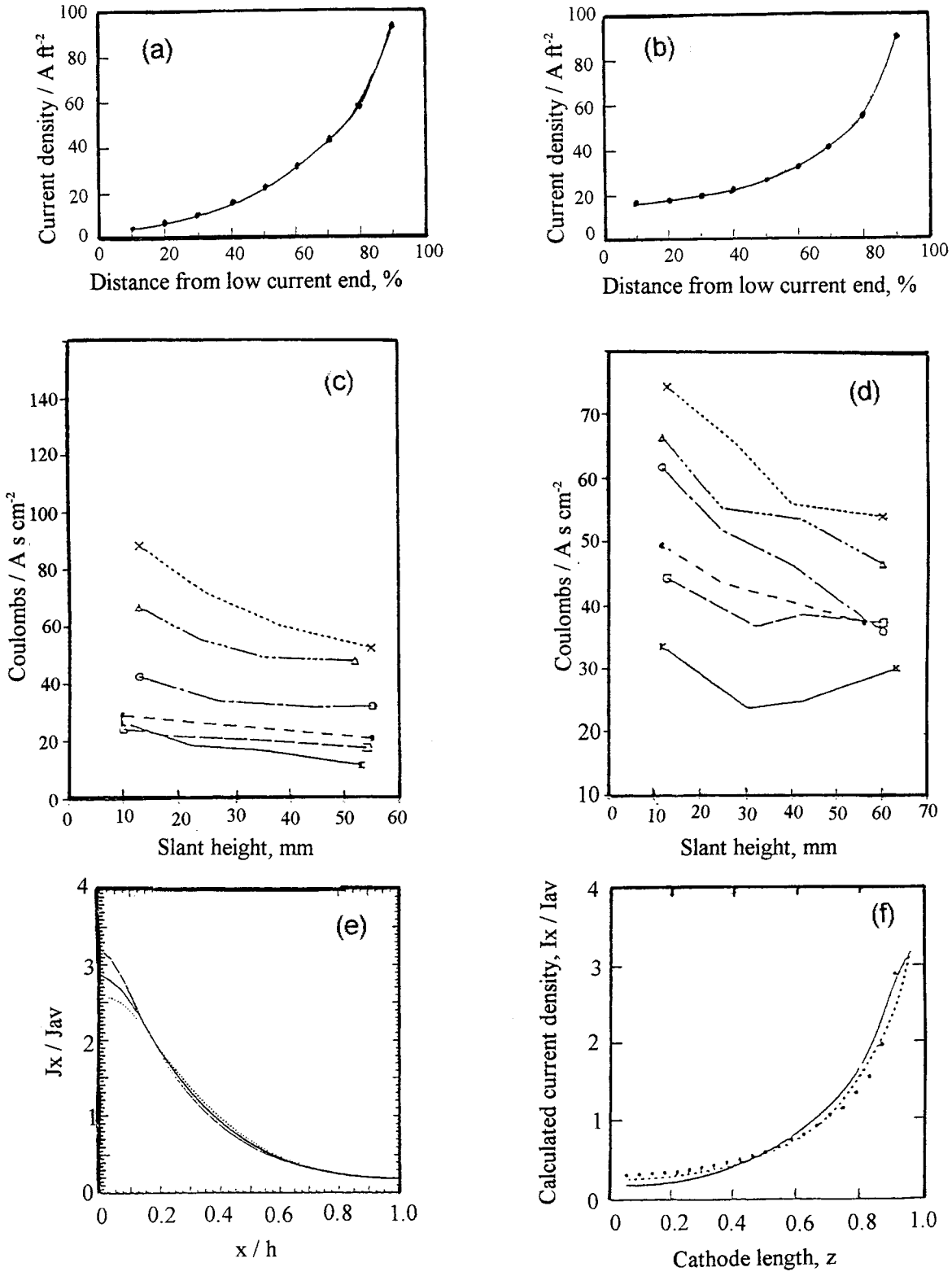

Fig. 16. Dynamic Hull cell correlations. (a), (b) Kadija *et al.* [145]; (c), (d) Afshar *et al.* [141]; with rotation rates: (⊗) 0, (□) 30,(●)50, (○) 100, (△) 200 and (×) 300rpm; (e) Madore *et al.* [137, 138]; with b/c (·····) 0.3, (– – –) 0.5 and (——) 0.9; (f) Madore *et al.* [137, 138]; with copper thickness (●), secondary distribution (·····) and Equation (——).

Since that time a number of studies have been reported under three distinct categories:

(i) use of the RCE for simulation of flow and agitation in corrosion including the superimposition of secondary agitation (e.g., jetting)
(ii) mathematical modelling and quantitative simulation or correlation
(iii) exploitation of RCE turbulence in erosion corrosion

The whole subject of flow-induced corrosion has been separately reviewed by Weber [146] and Poulson [147].

An important step has been taken by several workers who have shown the feasibility of coupling a RCE mass transfer controlled corrosion situation with other corrosion techniques including Stern–Geary analysis [148], impedance spectroscopy measurements [149–156] Weber [146] has rightly emphasized that corrosion processes may involve a number of mass transport stages which can each be rate-controlling:

(i) delivery of reactants to the anodic site
(ii) removal of products from the anodic site
(iii) analogous mass transfer at the cathodic site
(iv) property changes due to anodic film repair or breakdown.

These roles may be manifested in a series of corrosion rate (mass transfer coefficient) relationships with flow rate (rotation rate), see Fig. 17.

Many of the corrosion studies reported are very specific and include other aspects as part of the larger study; thus, the effect of pH on dissolution of calcite in a mineralogical context was reported by Compton *et al.* [163] and on synthetic minewater by Cheers [158]. The superimposed effects of aeration and consequent oxygen reduction has been considered by Silverman [164] and Mansfeld *et al.* [152] and Kolman and Taylor [168]. Similarly, classical chemical engineering problems of concentrated acid attack in plant [161] and galvanic corrosion [160] have been reported (Table 5).

One particularly discordant note has been struck by Brown *et al.* [162] who, in studying ozonated brine attack of 304-type stainless steel, have suggested a critical Reynolds number of 1900 (the usual value being about 200) which they claim is substantiated by Mallock [173]. However, the surface was subjected to passivation and repassivation by ozone and kinetic rather than mass transfer control might therefore have been responsible. Data from Silverman [161] illustrates this passivation effect (Fig. 18).

This discrepancy may be resolved by reverting to an older idea of utilizing the drag shear stress (see review [12] and a discussion of work by Theodorsen and Regier); Silverman [164] and Efird *et al.* [175] have expressed it as

$$\tau_W = 0.0791\, Re^{-0.3} \rho r^2 \omega^2 \qquad (15)$$

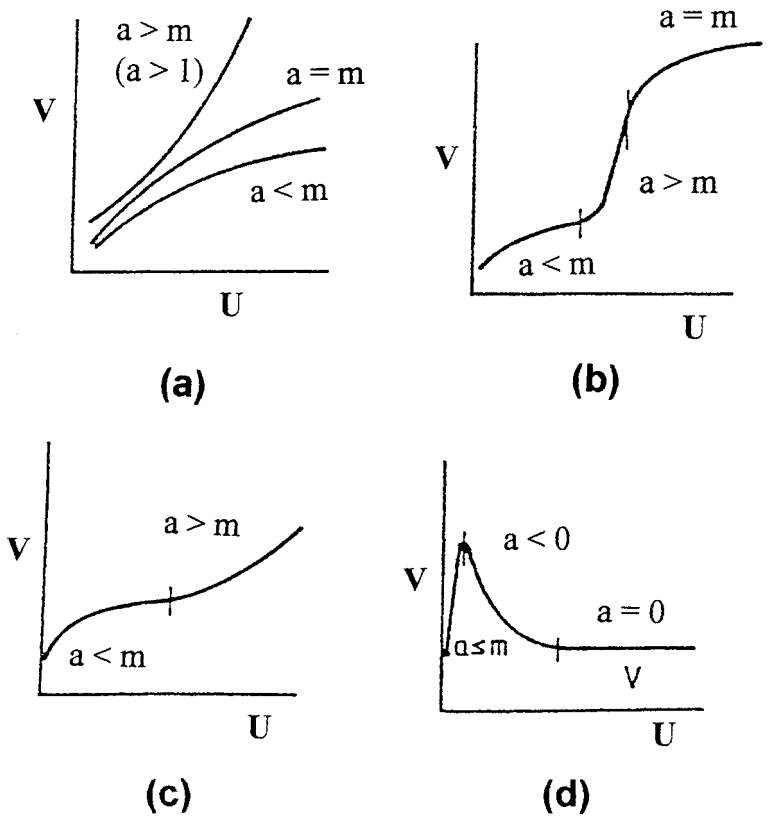

Fig. 17. Schematic dependence of corrosion rate (v) on flow rate (u) assuming a power law behaviour, $v = u^a$. (a) Pure transport control where a = m, a < m, a > m; (b) transport control followed by film formation and a dissolution region; (c) transport control and substrate wear; (d) transport control and passive film limiting dissolution.

Table 5. Corrosion processes and the RCE

Corrosion reactions	
CO_2 corrosion in oil wells	Denpo and Ogawa [148]
Steel in sea water	Holser *et al.* [157]
Mild steel in synthetic minewater	Cheers [158]
Pipelines	Sedahmed *et al.* [159]
Galvanic corrosion in seawater	Mansfeld and Kenkel [160]
Ni–Zn–P alloys	Swathirajan [118]
E Brite 26-V in conc. H_2SO_4	Silverman and Zerr [161]
304 stainless steel in ozonated NaCl	Brown *et al.* [162]
Calcite dissolution in aqueous solutions	Compton *et al.* [163]
90Cu–10Ni alloys in NaCl	Chen *et al.* [150]
Oxygen reduction	
On Cu–Ni alloy in NaCl and Na_2SO_4	Silverman [164]
Neutral aerated media	Mansfeld *et al.* [151, 153]
Anode dissolution	
Dissolution in fused salts	Leistra and Sides [165, 168]
Inhibitor behaviour	
Na_2MoO_4 for mild steel in natural waters	Kolman *et al.* [168]
Use of drag reducing agents	Sedahmed *et al.* [169]
Superimposed jetting	
Passive film persistency	Esteban *et al.* [170]
Surface cleansing	Noninski [171]
Steel corrosion	Efird *et al.* [172]

This equation is especially valid in the context of surface microroughness and is perhaps an appropriate approach in this consideration of film passivation and breakdown which defines the laminar-turbulent transition for $200 < Re < 2000$ when Taylor vortices are developing and which are necessarily sensitive to surface film imperfections.

The drive to create good mathematical models for corrosion studies is essentially to exploit the RCE as a compact laboratory simulation tool for a variety of industrial flow situations not otherwise convenient or suitable for laboratory modelling. Perhaps the first to attempt the correlation were Wranglen *et al.* [99] who used mass transfer equivalence through common Sherwood (or Nusselt) numbers thereby equating pipe flow and cylinder rotation by

$$\log Re_{\text{tube}} = 0.670 + 0.833 \log Re_{\text{cyl}} \qquad (16)$$

Poulson [147] broadly followed this approach but recommended care in its use for a number of cited situations including instances of inadequately developed turbulent flow and the presence of passive films on stainless steel. Silverman [164, 174] has also explored this approach and presented data to justify its adoption highlighting again the difficulties with film-forming alloys, but reaffirming the value of the RCE in studying velocity-sensitive corrosion. Holser *et al.* [157] have equated i_L values and used the technique to determine concentration of dissolved oxygen, viscosity and diffusion coefficient values. Chen *et al.* [150] have described the most rigorous study to date with the collation of a large amount of experimental data.

Jackson *et al.* [135, 136] have used the same approach for continuous strip plating in the production of electrolytic tinplate in which they have equated mass transfer coefficients for a turbulent plating line to a laboratory RCE simulation cell. Initial results indicate a good correlation thus justifying the long-standing practice in this industry.

The problem of erosion is one of dubious connection with mass-transfer controlled corrosion because it is often a problem of cavitation or momentum damage induced at high levels of turbulent flow. However, Weber [146] has attempted to discuss the relation of corrosion to erosion and has shown how erosion may be 'inhibited' by the use of drag-reducing additives and surfactants which act as shear friction lubricants and not as electrochemical inhibitors in the classical manner. He has emphasized further that erosion and cavitation resistance is primarily a function of metal surface hardness and microstructure and the RCE is therefore merely a means of changing the surface shear stresses. Heitz [175] recognized many years ago that the RCE geometry, having a low critical Reynolds number, was peculiarly advantageous for erosion simulation but surprisingly little research appears to have taken place on this important topic. In fact, some authors have reverted to the RDE (e.g., Sanchez and Schiffrin [176]). Substantial opportunities exist in this field.

Mercer and Lumbard [177] have described an apparatus for determining the corrosion behaviour of carbon steel in various waters. An RCE assembly was used to provide controlled flow conditions and to establish a constant dissolved oxygen concentration. Long term (~150 day) tests were carried out at 5–90 °C in triply-distilled water, water containing 35 ppm Cl^-, Teddington tap water and sea water. The RCE consisted of 15 mm diameter, 40 mm long, hollow tubes held between PTFE end caps with rotation speeds in the range 0–120rpm. The test apparatus was constructed entirely in PTFE to avoid

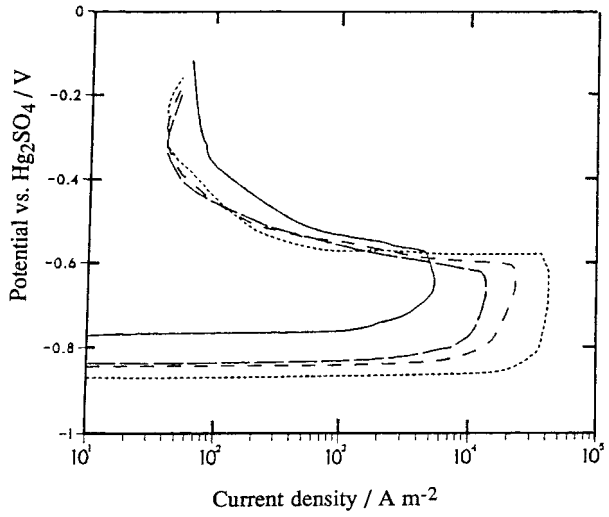

Fig. 18. Polarization curves for E-Brite stainless steel in industrial grade 93% sulphuric acid at 333 K, showing the effect of RCE rotation rate. After Silverman [174]. Rotation rates: (- - - - -) 0, (---- ----) 20.9, (-- -- --) 52.0 and (·····) 209 rod s^{-1}.

electrolyte contaminants arising from the leaching of silica in glass apparatus.

Nesic, Solvi and Enerhaug [178] have studied corrosion using simultaneously the RCE and pipe flow systems in the same flow loop. Comparisons were carried out in purified water at 20–80°C, pH 4–6, 0–1 bar CO_2 partial pressure and an electrode/electrolyte relative velocity of 0–13 m s^{-1}. The range of flow velocity covered a range of hydrodynamic conditions from static flow through to fully developed turbulent flow. Good agreement between experimental measurements and literature correlations due to Eisenberg Tobias and Wilke [25, 26] and Theodorsen and Regier (see [12]) was found.

8. Conclusions

The RCE has now established itself as a major tool for studying electrochemical mass transport especially under turbulent conditions. During the 15 years which have elapsed since the subject was last reviewed, over 100 applications have been recorded in a number of fields and the versatility of the RCE has been fully demonstrated.

References

[1] V. G. Levich, 'Physiochemical Hydrodynamics', Prentice-Hall, New York (1962).
[2] A. C. Riddiford, *Adv. Electrochem. & Electrochem. Eng.* **98** (1966) 309.
[3] R. N. Adams, 'Electrochemistry at Solid Electrodes', Dekker, New York (1969).
[4] W. J. Albery and M. L. Hitchman, 'Ring-Disc Electrodes', OUP Oxford (1971).
[5] Yu. V. Pleskov and V. Yu. Filinovskii, 'The Ring Disc Electrode', Consultants Bureau, New York (1976).
[6] C. M. A. Brett and A. M. C. F. Oliveira Brett, 'Comprehensive Chemical Kinetics' (edited by C. H. Bamford and R. G. Compton), **26**, Elsevier, Amsterdam, (1986).
[7] A. A. Wragg, 'The Chemical Engineer' (1977), p. 39.
[8] Idem, *J. Appl. Electrochem.* **21** (1991) 1047.
[9] J. R. Selman and C. W. Tobias, *Adv. Chem. Eng.* **10** (1978) 211.
[10] U. Landau. *A. I. Ch. E. Symp. Ser.* **77** (1981) 75.
[11] D. R. Gabe and P. A. Makanjuola. *I. Chem. E. Symp. Ser.* **98** (1986) 309.
[12] D. R. Gabe. *J. Appl. Electrochem.* **4** (1974) 91.
[13] D. R. Gabe and F. C. Walsh. *ibid.* **13** (1983) 3.
[14] H. Ohba and S. Kuroda, *JSME International J., Ser B* **36** (1993) 592.
[15] R. C. DiPrima and H. L. Swinney, *in* 'Hydrodynamic Instabilities and the Transition to Turbulence' (edited by H. L. Swinney and J. P. Gollub), Springer-Verlag, Berlin (1985), p. 139.
[16] Y. Takeda, W. E. Fischer and J. Sakakibara, *Science* **263** (1994) 502.
[17] D. Andereck, S. S. Liu and H. L. Swinney, *J. Fluid. Mech.* **164** (1986) 155.
[18] V. Sobolik, B. Benabes and G. Cognet, *J. Appl. Electrochem.* **25** (1995), 441.
[19] T. J. Hanratty and J. A. Campbell, *in* 'Fluid Mechanics Measurements' (edited by R. J. Goldstein), Hemisphere, Washington DC, (1983), p. 559.
[20] V. Sobolik, B. Benabes and G. Gognet, Progress and Trends in Rheology IV, Proceedings of the 4th European Rheology Conference (edited by C. Gallegas), Sevilla (1994), p. 551
[21] F. Walsh, 'A First Course in Electrochemical Engineering, The Electrochemical Consultancy', Romsey (1993).
[22] *Idem*, The role of the rotating cylinder electrode reactor in metal ion removal, *in* 'Electrochemistry for a Cleaner Environment' (edited by J. D. Genders and N. Weinberg), The Electrosynthesis Company Inc, E. Amherst, NJ (1992), chapter 4.
[23] D. R. Gabe, *Plat. Surf. Finish.* **82** (9) (1995) 69.
[24] R. A. Scannell and F. C. Walsh, *I. Chem. E. Symp. Ser.* **112** (1989) 222.
[25] M. Eisenberg, C. W, Tobias and C. R. Wilke, *J. Electrochem. Soc.* **101** (1954) 306.
[26] M. Eisenberg, C. W. Tobias and C. R. Wilke, *Chem. Eng. Prog. Symp. Ser.* **51** (1995) 1.
[27] D. J. Robinson and D. R. Gabe, *Trans. Inst. Metal Finish.* **48** (1970) 35; *ibid.* **49** (1971) 17.
[28] D. R. Gabe and P. A. Makanjuola, *I. Chem. E. Symp. Ser* **96** (1983) 221.
[29] *Idem*, *J. Appl. Electrochem.* **17** (1987) 370.
[30] D. R. Gabe and F. C. Walsh, *J. Appl. Electrochem.* **15** (1985) 807.
[31] N. A. Gardner and F. C. Walsh, *in* 'Electrochemical Cell Design', (edited by R. E. White) Plenum Press, New York (1984), p. 225.
[32] D. R. Gabe and F. C. Walsh, *Surf. Technol.* **12** (1981) 25.
[33] F. C. Walsh, PhD thesis, Loughborough University of Technology (1981).
[34] D. R. Gabe and F. C. Walsh, *J. Appl. Electrochem.* **14** (1984) 555.
[35] *Idem*, *ibid.* **14** (1984) 565.
[36] F. S. Holland, *Chem. Ind.* (*London*) (1978) 453.
[37] *Idem, UK patents 1 444 367* (1976) and *1 505 736* (1978); *US patent 4 028 199* (1977).
[38] G. Kreysa and Brandner, Proceedings of the 2nd World Congress on Chemical Engineering, Montreal (Oct. 1981); G. Kreyser, *Electrochim Acta* **26** (1981) 1693.
[39] A. H. Nahle, G. W. Reade and F. C. Walsh, *J. Appl. Electrochem.* **25** (1995) 450.
[40] F. C. Walsh, N. A. Gardner and D. R. Gabe, *ibid.* **12** (1982) 299.
[41] MVH Cell, van Aspert bv, Kastanjeweg 68, 5401 JP, Uden, The Netherlands.
[42] J-Cl. Puippe, *Oberflach. Surf.* **32** (2) (1991) 17; EAST Report (1990), 38, E. G. Leuze Verlag. Saulgau, Germany; *Galvano-Organo-Traitments de Surface* **61** (1992) 259.
[43] D. Hemsley, *Prod. Fin.* **46** (9) (1993) 5; *idem*, *ibid.* **47** (5), (1994), 6; *idem*, *ibid.* **47** (7), (1994), 9.
[44] M. Mayr, W. Blatt, B. Busse and H. Heinke, Electrolytic Systems for Applications in Fluoride-Containing, Electrolytes, Fourth International Forum on Electrolysis in the Chemical Industry, FA, 11–15 Nov. (1990).
[45] F. C. Walsh, The role of the rotating cylinder electrode reactor in metal ion removal, *in* 'Electrochemistry for a Cleaner Environment' (edited by J. D. Genders and N. L. Weinberg), The Electrosynthesis Company Inc., New York, (1992), chapter 4, p. 101.
[46] F. C. Walsh and D. R. Gabe, *I. Chem. E. Symp. Ser.* **116** (1990) 219.
[47] D. Anderston, M. Hanna, C. Ogden and D. Tench, *Plat. Surfa. Finish.* **70** (1983) 70.
[48] L. E. Vaaler, *J. Electrochem. Soc.* **125** (1978) 204.
[49] D. Robinson and F. C. Walsh, *Hydrometallurgy* **26** (1990) 115.
[50] *Idem*, *ibid.* **26** (1990) 93.
[51] F. C. Walsh, *ibid.* **33** (1993) 367.
[52] D. R. Gabe and F. C. Walsh, *Proc. Reinhardt Schuhmann Symp. Ser. Met. Soc.* (*AIME*) (1987) 774.
[53] D. Pletcher and F. C. Walsh, 'Industrial Electrochemistry', 2nd edn, Chapman & Hall, London (1990).
[54] F. C. Walsh and D. E. Saunders, *J. Photog. Sci.* **31** (1983) 35.
[55] D. Robinson and F. C. Walsh, *ibid.* **42** (1994) 1.
[56] F. C. Walsh, *I. Chem. E. Symp. Ser.*, No. 98 (1986) 137.
[57] A. C. Cooley, *J. Appl. Photogr. Eng.* **8** (1982) 171.
[58] *Idem*, *J. Imaging Technol.* **10** (1984) 226.
[59] F. C. Walsh, 'The Application of Rotating Cylinder Electrode Technology to Photographic Silver Recovery', *J. Phot. Sci.*, submitted.
[60] J. St-Pierre, N. Massé and M. Bergeron, *Electrochim. Acta.* **39** (1994) 2705.
[61] *Idem*, *ibid.* **40** (1993) 1013.
[62] N. Massé, J. St-Pierre and M. Bergeron, *J. Appl. Electrochem.* **25** (1995) 340.
[63] J. G. Sunderland and D. Tilston, *I. Mech. E. Seminar* (1993) 59.

[64] P. Adaikkalam, N. Sathaiyan and S. Visvanathan, *J. Chem. Tech. Biotechnol.* **56** (1993) 389.
[65] R. Gana, M. Figueroa, L. Kattan, I. Moller and M. A. Esteso, J. *Appl. Electrochem.* **25** (1995) 1052.
[66] R. Gana, M. Figueroa, L. Kattan, J. M. Sanchez and M. A. Esteso, *ibid.* **25** (1995) 240.
[67] J. C. Farmer, Electrochemical treatment of mixed and hazardous wastes, *in* 'Environmental Oriented Electrochemistry' (edited by C. A. C. Sequeira), Elsevier, Amsterdam, (1994), p. 565.
[68] H. V. K. Udupa and K. S. Udupa, Use of rotating electrodes for small-scale electroorganic processes, *in* 'Technique of Electroorganic Synthesis – Scale-up and Engineering Aspects' (edited by N. L. Weinberg and B. V. Tilak), Vol. V, part III, J. Wiley & Sons, New York (1982), chapter 8, p. 385.
[69] Z. Stankovic and M. Rajcic-Vujasinovic, *Khem. Ind.* **38** (1984) 337.
[70] A. Eklund and D. Simonsson, *J. Appl. Electrochem.* **18** (1988) 710.
[71] F. C. Walsh, unpublished work; C. C. Blake and C. C. O. Goodall, *European Patent 084 521, 83 810 0 13.9* (1983) (to Ciba-Geigy).
[72] Z. Tomczuk, W. E. Miller, R. D. Wolson and E. G. Gay, *US Patent 5 009 752*, 23 Apr. (1991) (to US Department of Energy).
[73] A. Schymalla and M. Baeseler, *Chemische Technik* **42** (1990) 514.
[74] P-C. Cheng, T. Nonaka and T-C. Chou, *Bull. Chem. Soc. Jpn.* **64** (1991) 1911.
[75] P-C. Cheng and T. Nonaka, *Denki Kagaku* **61** (1993) 218.
[76] G. Johansson, *Talanta* **12** (1965) 163.
[77] J. W. Burgman and P. J. Sides, *Electrochim. Acta* **34** (1989) 841.
[78] J. Vanhumbeeck. A. E. F. S. Annual Conference (1984).
[79] R. deDoncker and J. Vanhumbeeck. Proc. 'Connectors 85' Conference, 63.
[80] T. C. van Vechten, D. S. Lashmore, C. E. Johnson and J. Cl. Puippe. *Plating Surf. Fin.* **83(12)** (1986) 45.
[81] P A Makanjuola and D. R. Gabe, *Surfa. Technol.* **24** (1985) 29.
[82] K. R. Wehmeyer, M. R. Denkin and R. M. Wightman, *Anal. Chem.* **57** (1985) 1913.
[83] W. Thormann, P. van den Bosch and A. M. Bond, *ibid.* **57** (1985) 2764.
[84] H. Deligianni and L. T. Romankiw, *I. B. M. J. Res. Dev.* **37** (1993) 85.
[85] P Hildebrandt, K. A. Malor and R. S. Czernvszewick, *J. Raman Spectrosc.* **19** (1988) 65.
[86] B. Morrison, K. Striebel, P. N. Ross and P. C. Andriacos, *J. Electroanal. Chem.* **215** (1986) 151.
[87] D. Pletcher, 'A First Course in Electrode Processes', The Electrochemical Consultancy, Romsey (1991).
[88] D. T. Sawyer, A Sobkowiak and J. L. Roberts, Electrochemistry for Chemists, Wiley-Interscience, New York, (1995), p. 270.
[89] E. Farndon, S. A. Campbell and F. C. Walsh, *J. Appl. Electrochem.* **25** (1995) 574.
[90] E. Farndon, E. Man, S. A. Campbell and F. C. Walsh, Paper presented at Interfinish 96, Birmingham, UK, 10–12 Sept. (1996).
[91] W. J. Blaedel and J. Wang, *Electrochim. Acta* **52** (1980) 1697, 1724.
[92] G. W. Reade, PhD thesis, University of Portsmouth. UK (1996).
[93] H. Reller, I. Feldstein-Hallakoun and E. Gileadi, *Electrochim. Acta* **33** (1988) 95.
[94] F. C. Walsh, unpublished work.
[95] M. Fleischmann, S. Pons, D. R. Rolison and P.P, Schmidt (Eds), 'Ultramicroelectrodes', Datatech Systems, Morganton, VA (1987)
[96] F. C. Walsh and D. R. Gabe, *Trans. I. Chem. E.* **68B** (1990) 107.
[97] D. R. Gabe and F. C. Walsh, Design considerations for rotating cylinder electrode reactors, Summer National Meeting of The AIChE, Electrochemical Engineering Aspects of Electroplating Symposium, Cleveland, Ohio, 29 Aug.– 1 Sept. (1982); Electrochem. Soc. Symp., **83-12**, 'Electroplating Engineering and Waste Recycle-New Developments and Trends' (edited by D. Snyder, U. Landau and R. Sard), The Electrochemical Society, pp. 367–83.
[98] R. de Doncker and J. Vanhumbeeck, *Trans. Inst. Met. Finish.* **62** (1985) 59.
[99] D. A. Swalheim, *Trans. Electrochem. Soc.* **86** (1944) 395.
[100] G. Wranglen, J. Berendson and G. Karlberg, *in* 'Physico-Chemical Hydrodynamics' (edited by B. Spalding) Adv. Pubs., London (1977).
[101] R. Winand, *Electrochim. Acta* **39** (1994) 1091.
[102] R. D. Naybour, *ibid.* **13** (1968) 763.
[103] S. Alota and N. Azzerri, Proc. SURTEC 85, Berlin (1985) 367.
[104] J. Vanhumbeeck, Proc. AEFS SURFIN '84, Session C (1984).
[105] A. Tseda *et al.*, Proc. AEFS SURFIN '84, Session C, (1984)
[106] D. R. Gabe and G. D. Wilcox, unpublished work.
[107] K. J. Cathro, *J. Electrochem. Soc.* **139** (1992) 2186.
[108] A. K. Graham and H. L. Pinkerton, *Proc. Amer. Electroplaters Soc.* **50** (1963) 135.
[109] C. Madore, M. Matlosz and D. Landolt, *J. Appl. Electrochem.* **22** (1992) 1155.
[110] D. R. Gabe, Asia-Pacific Interfinish Conference Melbourne, Oct. (1994), Plenary Lecture.
[111] G. Devaraj, G. N. K. Ramesh Bapu, J. Ayyaparaju and R. Subramanian, *Bull. Electrochem.* **2**(1) (1986) 13.
[112] F. C. Walsh, Unpublished work.
[113] C. Ogden and D. Tench, Proc. AES/DES Finish Printed Wiring Hybrid Circuits, Winter Park FA. (1980) p. 1.
[114] C. Ogden, D. Tench and J. White, Proceedings of the 156th Meeting of the Electrochemical Society, Oct. (1979).
[115] W. D. Freitag, C. Ogden, D. Tench and J. White, *Plat. Surf. Finish.* **80**(10) (1983) 55.
[116] D. P. Barkey, R. H. Muller and C. W. Tobias, *J. Electrochem. Soc.* **136** (1989) 2199.
[117] *Idem*, *ibid.* **136** (1989) 2207.
[118] S. Swathirajan and Y. M. Mikhail, *ibid.* **136** (1989) 374.
[119] K. Sridharan and K. Sheppard, *Trans. Inst. Met. Finish.* **72** (1994) 153.
[120] D. Cruickshanks-Boyd, A. T. Kuhn and F. C. Walsh, *ibid.* **59** (1981) 68–72.
[121] A. T. Kuhn, P. Neufeld and K. Young, *J. Appl. Electcochem.* **14** (1984) 605.
[122] M. Schwartz, W. Li, N. H. Phan, K. Nobe and A. J. Pearlstein, *Surf. & Coatings Technol.* **52** (1992) 269.
[123] J. J. Dietrich, C. C. Liu, R. A. Powers and R. F. Savinell, Private communication.
[124] P. Kathirgamanathan and M. M. B. Qayyum, *J. Electrochem. Soc.* **141** (1994) 147.
[125] P. Kathirgamanathan, A. M. Souter and D. Baluch, *J. Appl. Electrochem.* **24** (1994) 283.
[126] S. Swathirajan and Y. M. Mikhail, *ibid.* **136** (1989) 2188.
[127] B. Sturzenegger and J. Cl. Puippe, *Plat. Met. Rev.* **28** (1984) 117.
[128] M. R. Kalantary, G. D. Wilcox and D. R. Gabe, *Electrochim. Acta* **40** (1995) 1609.
[129] M. Y. Foo, G. D. Wilcox and D. R. Gabe, *Proc Eur. Acad. Surf. Tech. Conf.,* Nov. (1993), p. 137.
[130] A. T. Kuhn, P. Neufeld and D. W. Cruickshanks-Boyd, *Trans. Inst. Met. Finish.* **61** (1983) 30.
[131] P. Neufeld, A. T. Kuhn and H. A. Skinner. Proc. Powtech. 83 Conf., *I. Chem. E. Symp. Ser.* **69** (1983) 71.
[132] A. Radwan, A. El-Kiar, H. A. Farag and G. H. Sedahmed, *J.Appl.Electrochem.* **22** (1992) 1161.
[133] G. H. Kelsall and P. W. Page, Electrochemical Society Spring Meeting., Cincinnati (1984), Abstr. 260.
[134] G. D. Wilcox and D. R. Gabe, Proc. Asia-Pacific Interfinish 94, Melbourne (1994), 50.1.
[135] A. C. Jackson, private communication (1996).
[136] A. C. Jackson, D. W. Bird and K. P. Williams, Proceedings of the AESF Conference on Strip Plating of Steel, Baltimore, May (1996).
[137] C. Madore, A. C. West, M. Matlosz and D. Landolt. *Electrochim. Acta* **37** (1992) 69.
[138] C. Madore and D. Landolt. *Plat. Surf. Finish.* **80**(11) (1993) 73.
[139] E. J. Podlaha, M. Matlosz and D. Landolt. *J. Electrochem Soc.* **140** (1993) L149.
[140] D. Reichenbach. *Plati. Surf. Finish.* **81**(5) (1994) 106.
[141] A. F. S. Afshar, D. R. Gabe and B. Sewell. *Trans. Inst. Met. Finish.* **69** (1991) 37.

[142] J. M. Bisang and G. Kreysa. *J. Appl. Electrochem.* **18** (1988) 422.
[143] D. R. Gabe and G. D. Wilcox. *Trans. Inst. Met. Finish.* **71** (1993) 71.
[144] Po-Yen Lu. *Plati. Surf. Finish.* **78**(10) (1991) 62.
[145] I. Kadija, J. A. Abys, V. Chinchankar and H. K. Straschil. *Plati. Surf. Finish.* **78**(7) (1991) 60.
[146] J. Weber, *Brit. Corr. J.* **27** (1992) 193.
[147] B. Poulson. *Corr.Sci.* **23** (1983) 391.
[148] K. Denpo and H. Ogawa, *Corrosion* **49** (1993) 442.
[149] D. C. Silverman. *Electrochim. Acta.* **38** (1993) 2075.
[150] T. Y. Chen, A. A. Moccari and D. D. MacDonald, *Corrosion* **48** (1992) 239.
[151] W. J. Lorenz and F. Mansfeld. Proceedings of the 8th International Congress on Metallic Corrosion, Mainz (1981) p. 2081.
[152] F. Mansfeld, M. W. Kendig and W. J. Lorenz. *J. Electrochem.Soc.* **132** (1985) 290.
[153] M. Shirkanzadhe, *Corrosion* **43** (1987) 621.
[154] M. Shirkanzadhe, *et al. Corr. Sci.* **27** (1987) 383, 1301.
[155] M. Shirkanzadhe, *Corr. Sci.* **28** (1988) 201.
[156] V. S. Akhomov, A. S. Abramov and A. V. Chekhovskii, *Prot. Metals USSR.* **23** (1987) 533.
[157] R. A. Holser, G. Prentice, R. B. Pond and R. Guanti, *Corrosion* **46** (1990) 764.
[158] P. V. Cheers, *J. South African Inst.Min.Met.* **92** (1992) 275.
[159] G. H. Sedahmed, B. A. Abdel-Naby and S. G. Tantawy, *Brit.Corr.J.* **25** (1990) 205.
[160] F. Mansfeld and J. V. Kenkel, *Corrosion* **33** (1977) 236.
[161] D. C. Silverman and M. E. Zerr, *ibid.* **42** (1986) 633.
[162] B. E. Brown, H. H. Lu and D. J. Duquette, *ibid.* **48** (1992) 970.
[163] R. G. Compton and P. R. Unwin, *Phil.Trans.Roy.Soc.,* Lond. **A330** (1990) 1.
[164] D. C. Silverman, *Corrosion* **40** (1984) 220.
[165] J. A. Leistra and P. J. Sides, *J. Metals* **37** (1985) 85.
[166] J. A. Leistra and P. J. Sides, *Light Metals* **2** (1986) 473.
[167] J. W. Burgman and P. J. Sides, *AIME Met. Trans.* **A121** (1987) 233.
[168] D. G. Kolman and S. R. Taylor, *Corrosion* **49** (1993) 622.
[169] G. H. Sedahmed, B. A. El-Naby and A. Abdel-Khali, *Corr.Sci.* **17** (1977) 865.
[170] J. M. Esteban, G. S. Hickey and M. E. Orazem, *Corrosion* **46** (1990) 896.
[171] V. C. Noninski, *Corr.Sci.* **30** (1990) 839.
[172] K. D. Efird, E. J. Wright, J. A. Boros and T. G. Hailey, *J. Electrochem. Soc.* **49** (1993) 992.
[173] A Mallock, *Proc.Roy. Soc. Lond.* **A187** (1986) 41.
[174] D. C. Silverman, *J. Electrochem. Soc.* **44** (1988) 42.
[175] E. Heitz, *Werkst. Korros.* **15** (1964) 63.
[176] S. R. de Sanchez and D. Schiffrin, *Corr. Sci.* **28** (1988) 141.
[177] A. D. Mercer and E. A. Lumbard, *Brit. Corr. J.* **30** (1995) 43.
[178] S. Nesic, G. T. Solvi and J. Enerhaug. *Corrosion* **51** (1995) 773.